Electromagnetic and neutral-current responses from Quantum Monte Carlo

Alessandro Lovato

In collaboration with:
Joe Carlson, Stefano Gandolfi, Diego Lonardoni, Juan Nieves, Maria Piarulli, Steve Pieper, Noemi Rocco, and Rocco Schiavilla

Istituto Nazionale di Fisica Nucleare

Argonne National Laboratory

NUCLEI Nuclear Computational Low-Energy Initiative

Why nuclear Physics is (again) cool?

- Atomic nuclei are strongly interacting many-body systems exhibiting fascinating properties including: shell structure, pairing and superfluidity, deformation, and self-emerging clustering.

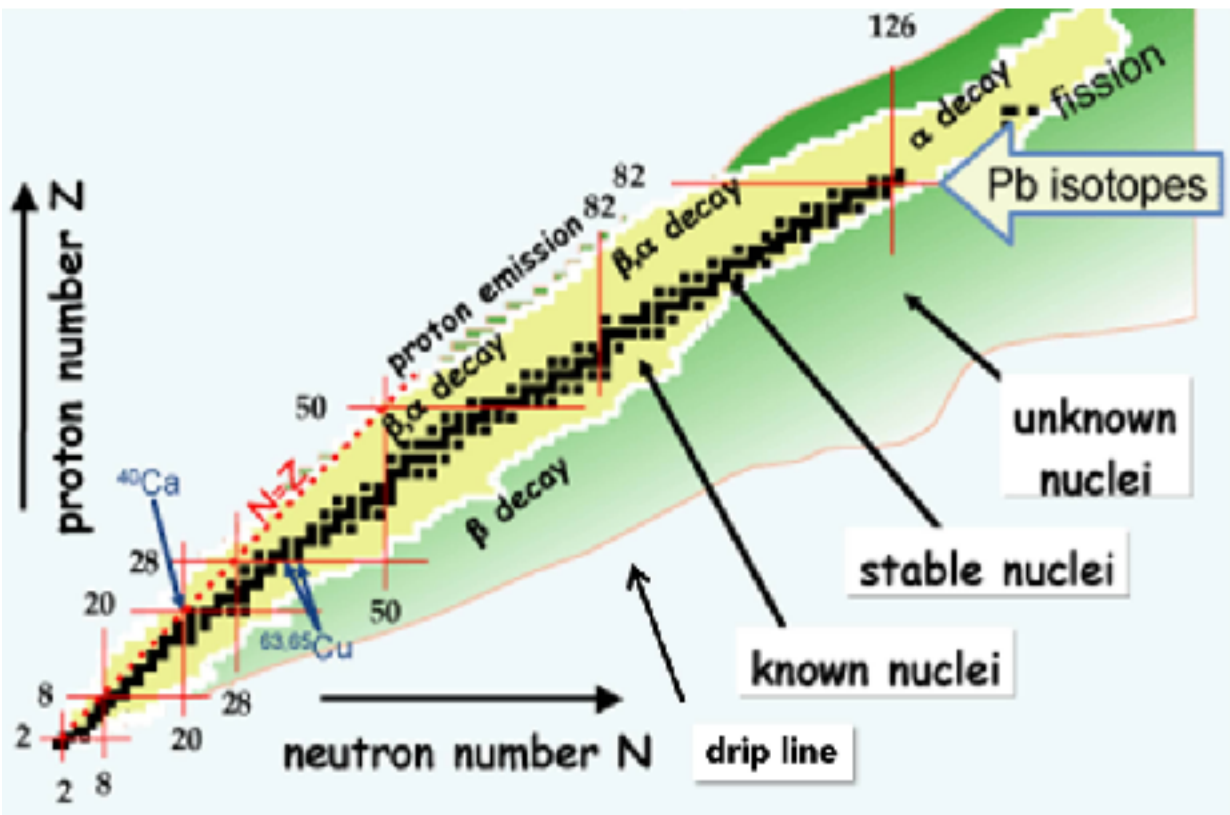

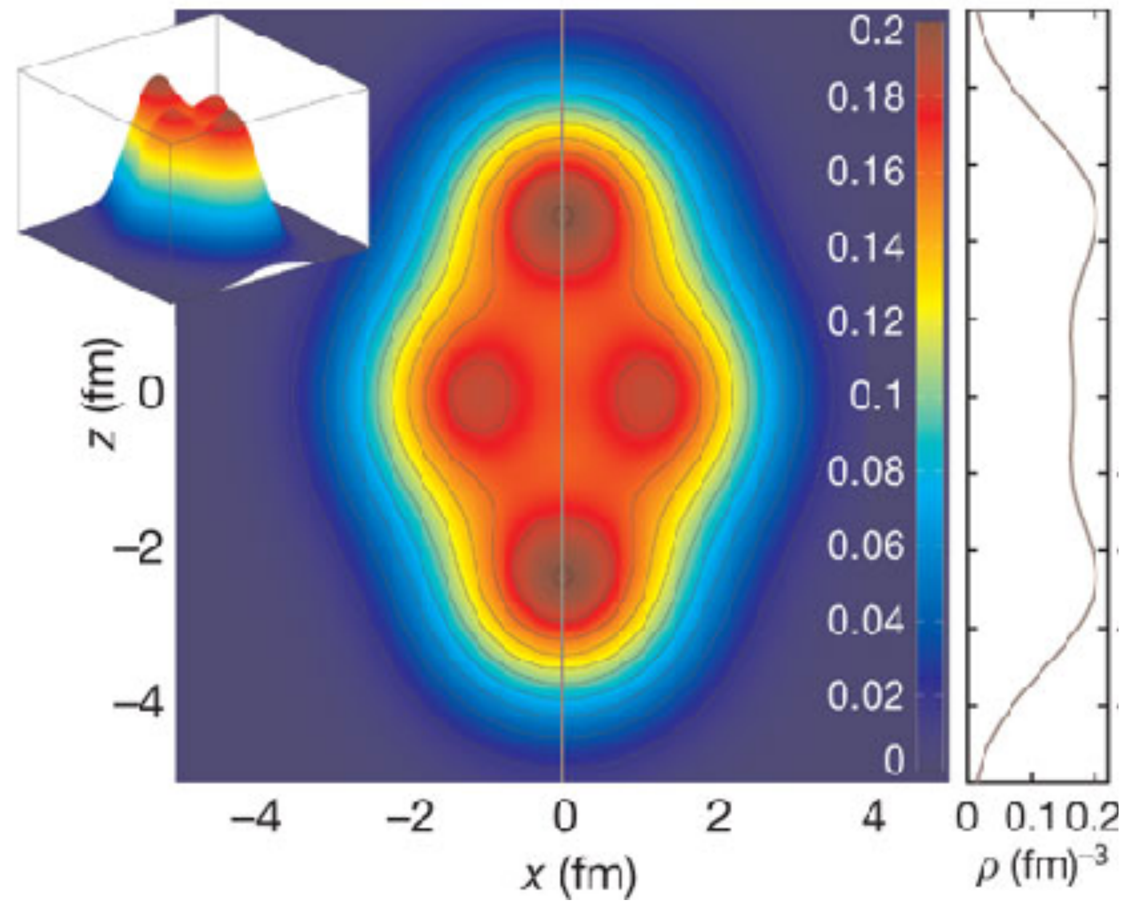

- Understanding their structure, reactions, and electroweak properties within a unified framework well-rooted in quantum chromodynamics has been a long-standing goal of nuclear physics.

QCD and the nuclear Hamiltonian

- Owing to its non-abelian character, QCD is strongly nonperturbative at “large” distances.

- Lattice-QCD is the most reliable way of “solving” QCD in the low-energy regime, and it promises to provide a solid foundation for the structure of nuclei directly from QCD

- The applicability of Lattice-QCD is limited to few body systems, (A<4), and to a nuclear physics in which the pion mass must be kept much higher than the physical one.

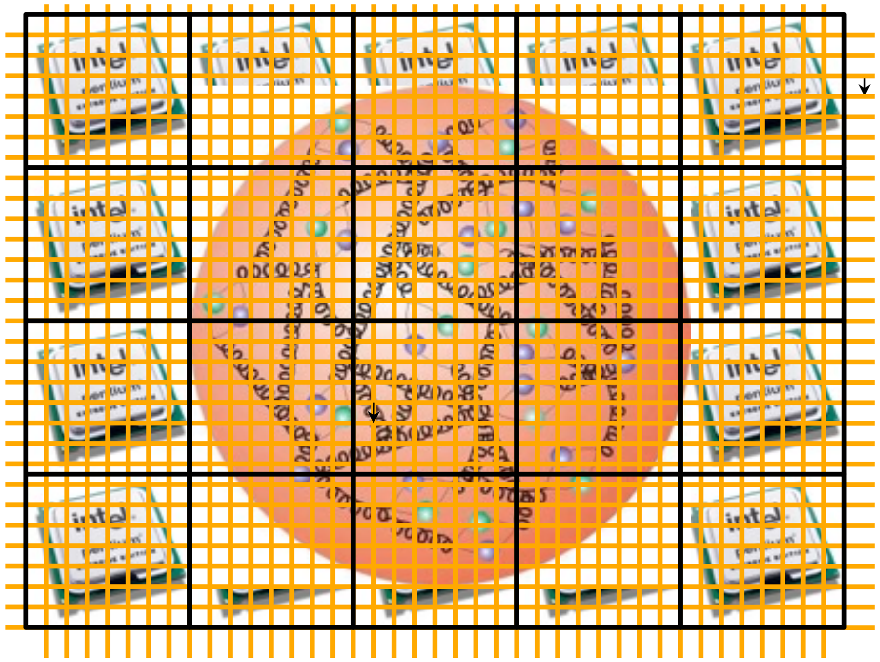

- Quark and gluons do not exists in the physical spectrum as asymptotic states

- Effective theory: non relativistic nucleons interacting via instantaneous potentials

$$H = \sum_i \frac{\mathbf{p}_i^2}{2m} + \sum_{i<j} v_{ij} + \sum_{i<j<k} V_{ijk} + \dots$$

Two-body potential

The Argonne v_{18} is a finite, local, configuration-space potential controlled by ~4300 np and pp scattering data below 350 MeV of the Nijmegen database

$$v_{18}(r_{ij}) = v_{ij}^{\gamma} + v_{ij}^{\pi} + v_{ij}^{I} + v_{ij}^{S} = \sum_{p=1}^{18} v^p(r_{ij}) O_{ij}^p$$

- Static part $O_{ij}^{p=1-6} = (1, \sigma_{ij}, S_{ij}) \otimes (1, \tau_{ij})$
- Spin-orbit $O_{ij}^{p=7-8} = \mathbf{L}_{ij} \cdot \mathbf{S}_{ij} \otimes (1, \tau_{ij})$

Some of the diagrams included in this potential are

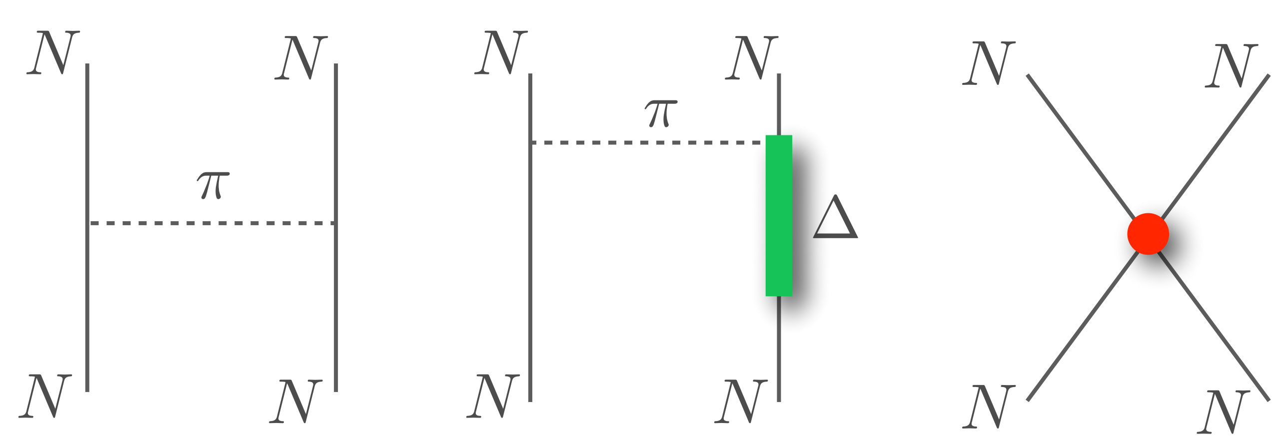

Three-body potential

An Hamiltonian which only includes Argonne v_{18} does not provide enough binding in the light nuclei and overestimates the equilibrium density of symmetric nuclear matter.

Three-body force is needed

Urbana IX
contains the attractive Fujita and Miyazawa two-pion exchange interaction and a phenomenological repulsive term.

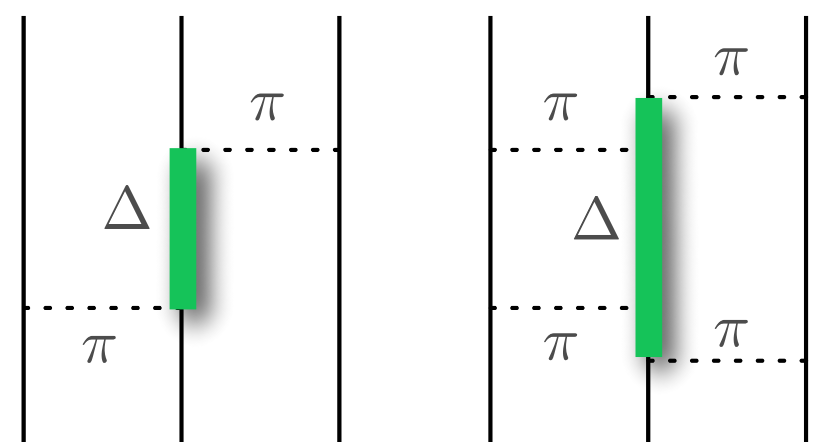

Illinois 7
also includes terms originating from three-pion exchange diagrams and the two-pion S-wave contribution.

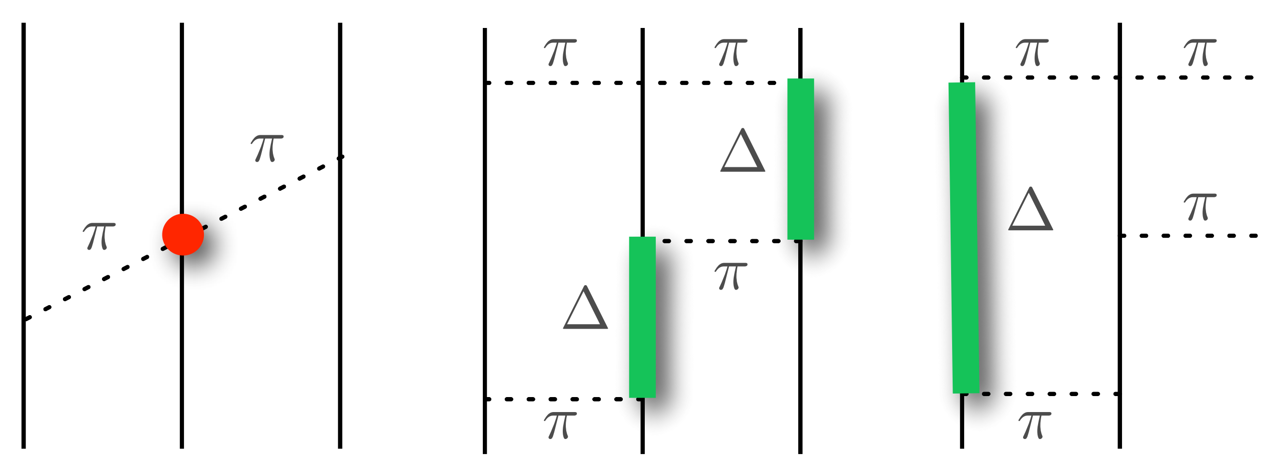

Nuclear currents

The nuclear electromagnetic current is constrained by the Hamiltonian through the continuity equation

$$\nabla \cdot \mathbf{J}_{\rm EM} + i[H, J^0_{\rm EM}] = 0$$

- The above equation implies that $\mathbf{J}_{\rm EM}$ involves two-nucleon contributions.

- They are essential for low-momentum and low-energy transfer transitions.

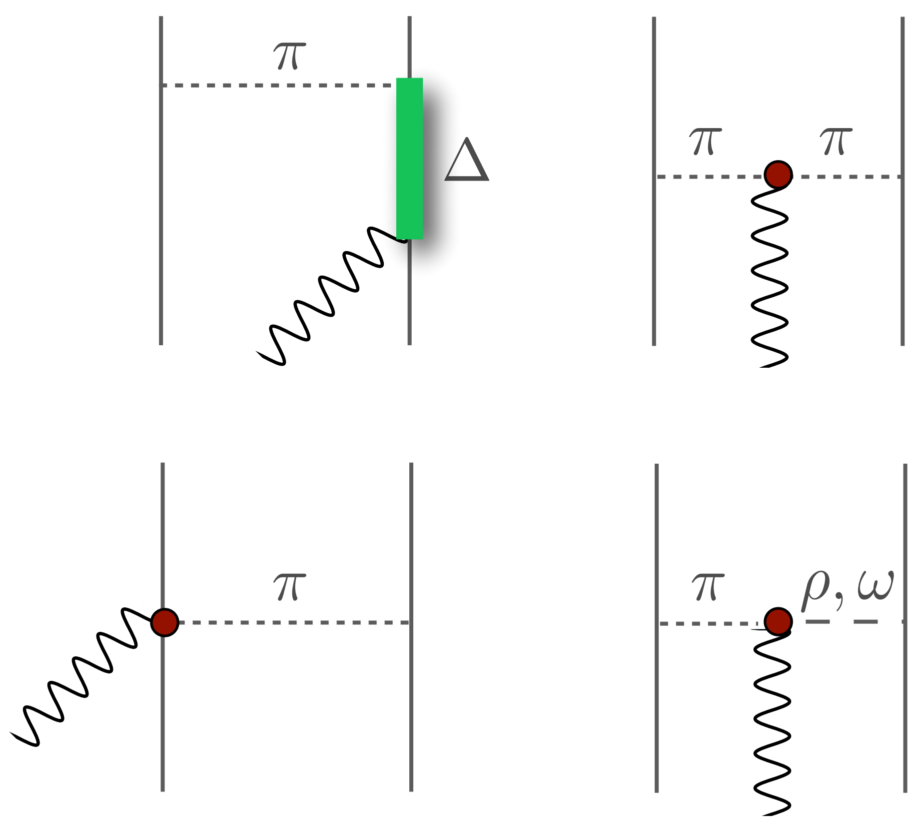

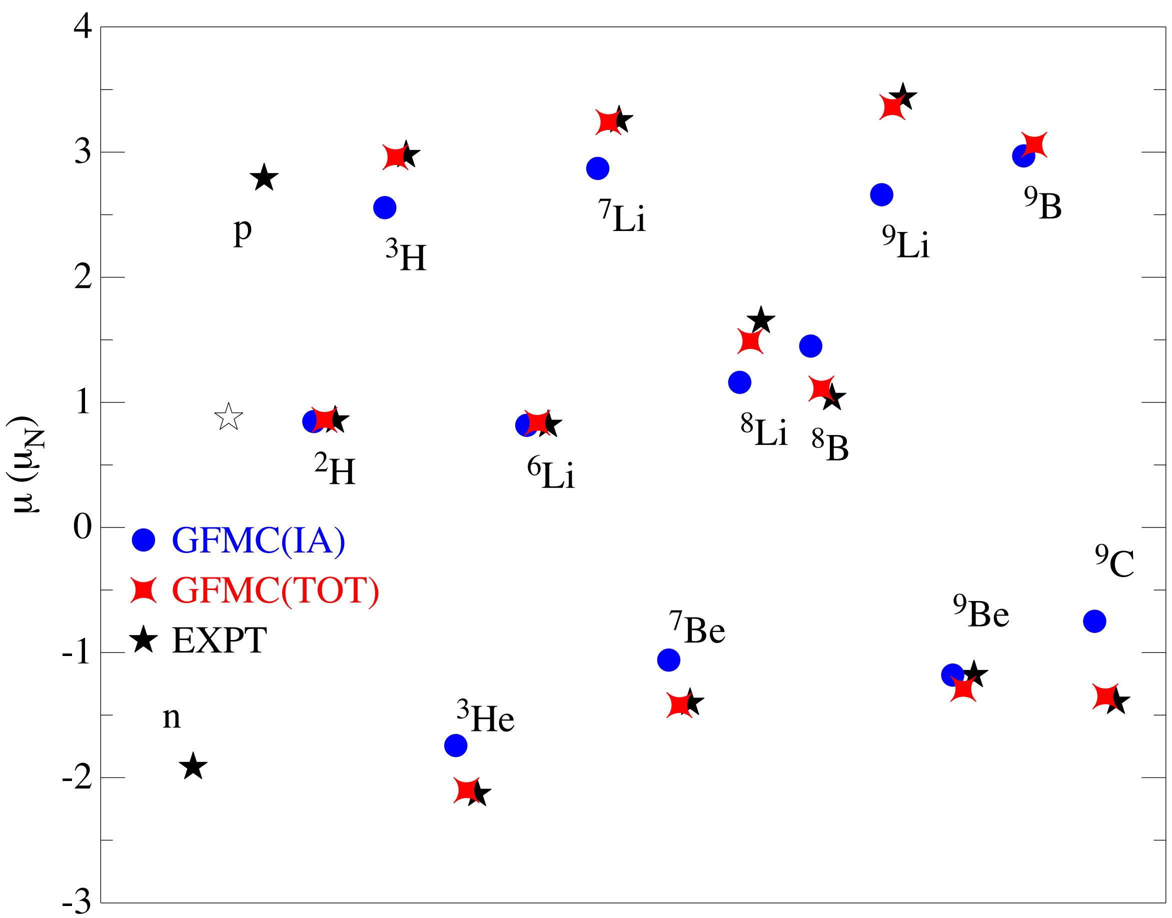

S. Pastore at al., PRC 87, 035503 (2013)

Why quantum Monte Carlo?

Quantum Monte Carlo provides a way to go from the nuclear hamiltonian to nuclear properties

$$H|\Psi_n\rangle = E_n|\Psi_n\rangle$$

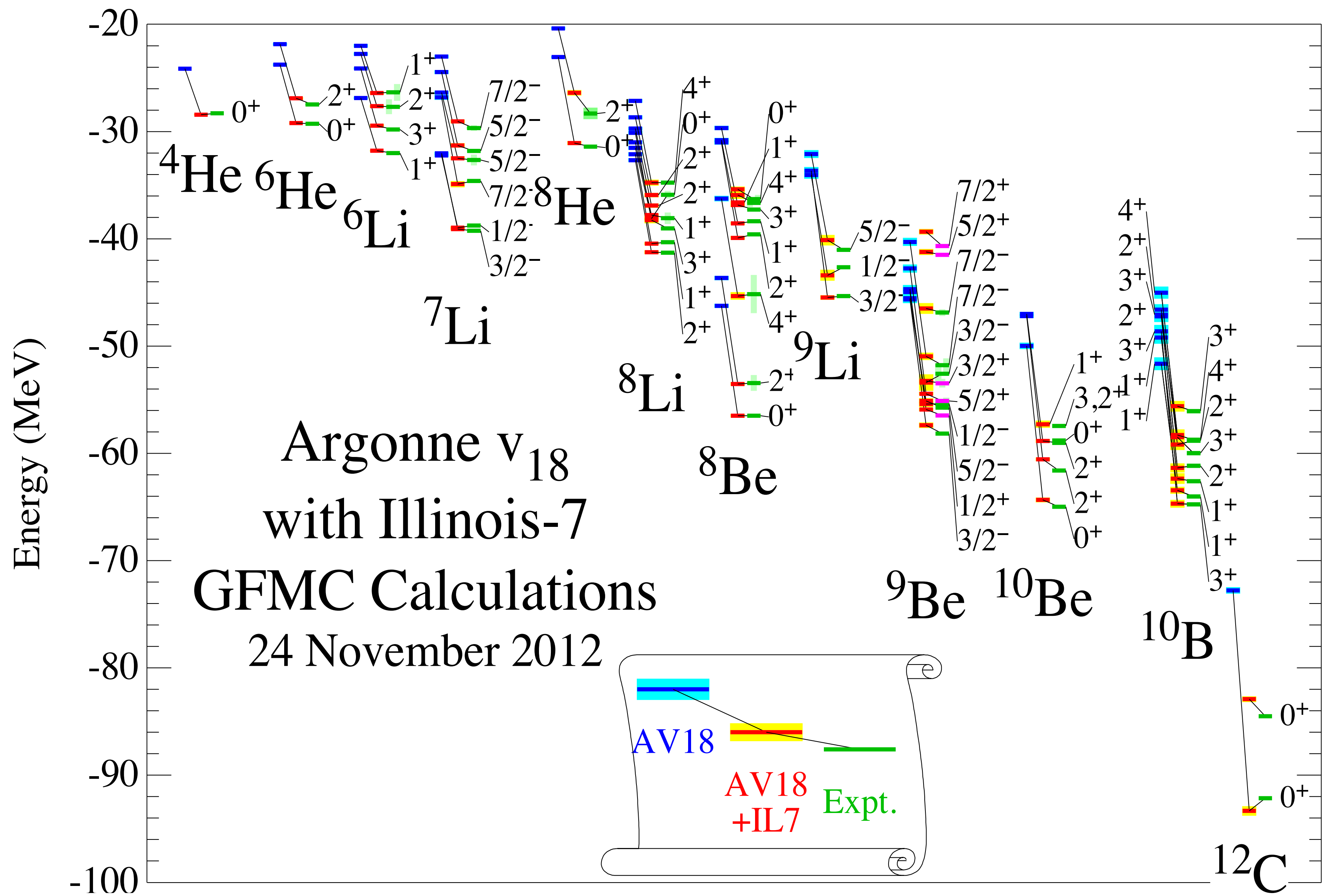

Lepton-nucleus scattering

The inclusive cross section of the process in which a lepton scatters off a nucleus can be written in terms of five response functions

$$\frac{d\sigma}{dE_{\ell'}d\Omega_\ell} \propto [v_{00}R_{00} + v_{zz}R_{zz} - v_{0z}R_{0z} + v_{xx}R_{xx} \mp v_{xy}R_{xy}]$$

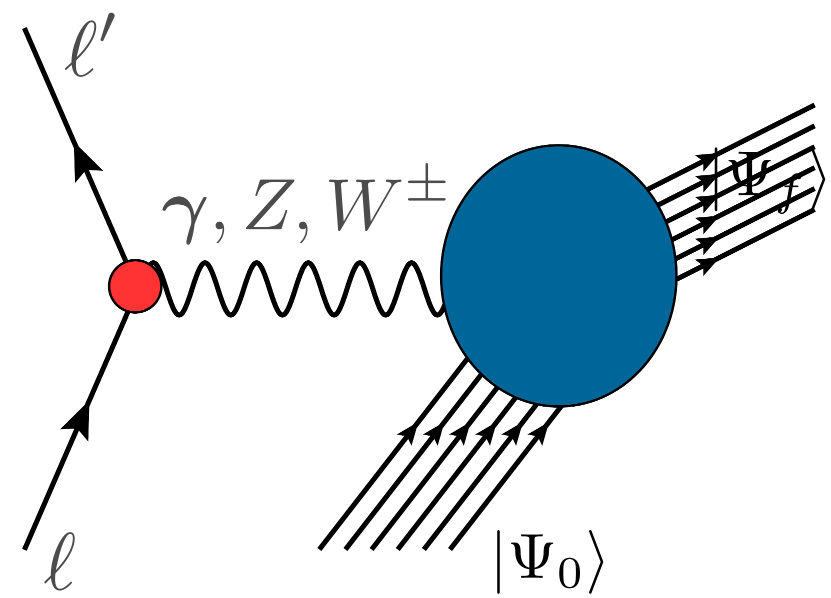

- In the electromagnetic case only the longitudinal and the transverse response functions contribute

- The response functions contain all the information on target structure and dynamics

$$R_{\alpha\beta}(\omega,\mathbf{q}) = \sum_f \langle\Psi_0|J^\dagger_\alpha(\mathbf{q})|\Psi_f\rangle\langle\Psi_f|J_\beta(\mathbf{q})|\Psi_0\rangle\delta(\omega - E_f + E_0)$$

- They account for initial state correlations, final state correlations and two-body currents

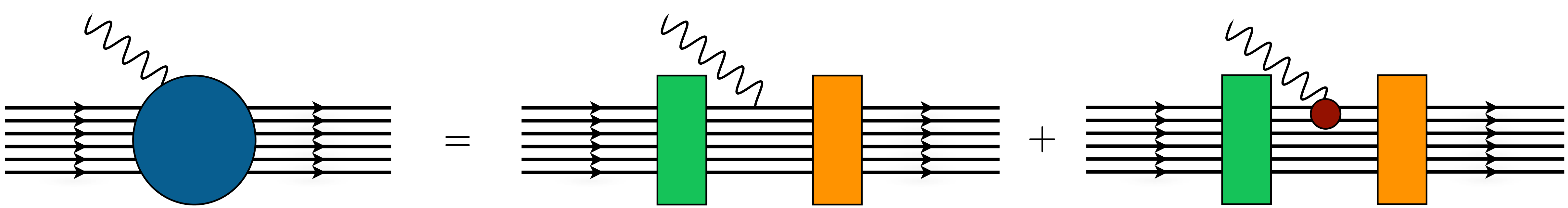

Lepton-nucleus scattering

- At (very) large momentum transfer, scattering off a nuclear target reduces to the sum of scattering processes involving bound nucleons → short-range correlations.

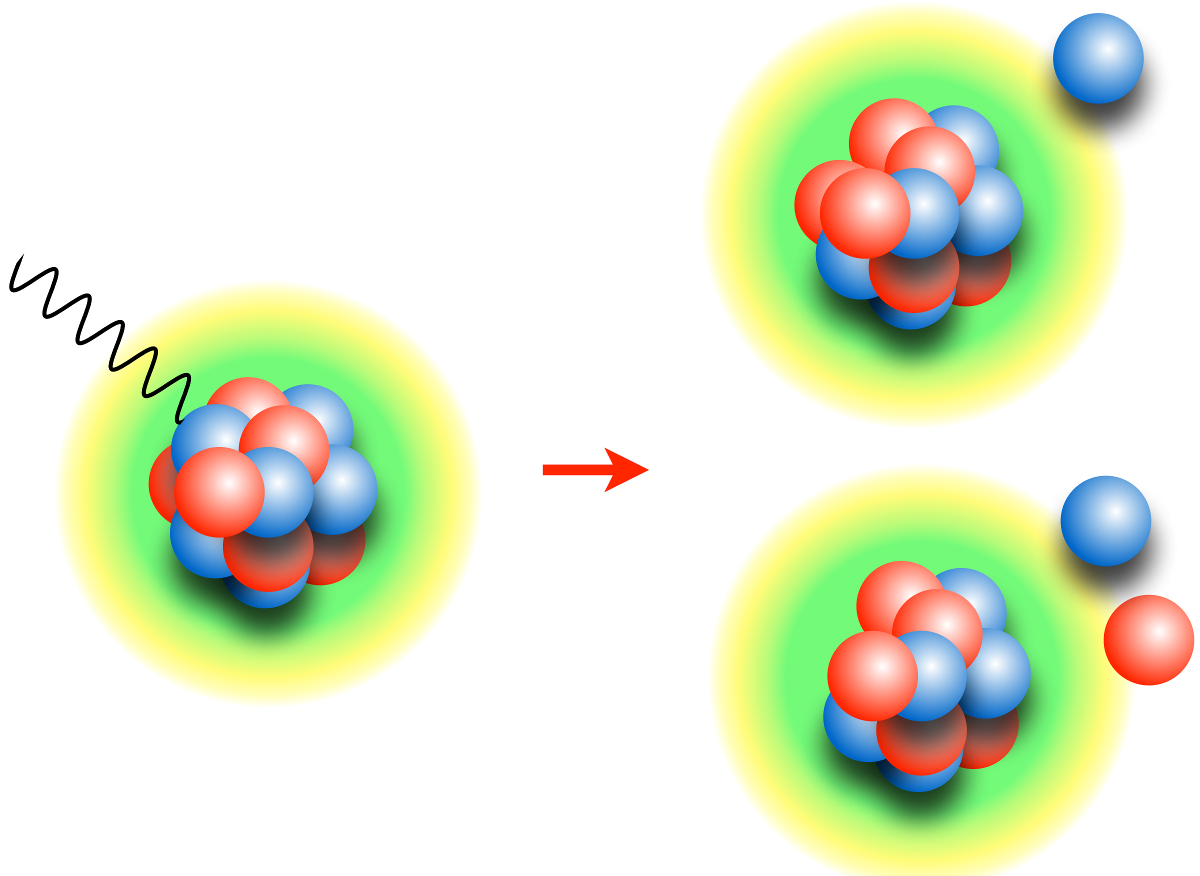

$$|\Psi_f\rangle \simeq |p_1\rangle \otimes |\Psi_f\rangle_{A-1}$$

$$|\Psi_f\rangle \simeq |p_1, p_2\rangle \otimes |\Psi_f\rangle_{A-2}$$

- Relativistic effects play a major role and need to be accounted for along with nuclear correlations (Non trivial interplay between them)

- Resonance production and deep inelastic scattering also need to be accounted for

Euclidean response function

Valuable information on the energy dependence of the response functions can be inferred from their Laplace transforms

$$E_{\alpha\beta}(\tau,\mathbf{q}) \equiv \int d\omega e^{-\omega\tau} R_{\alpha\beta}(\omega,\mathbf{q})$$

At finite imaginary time the contributions from large energy transfer are quickly suppressed

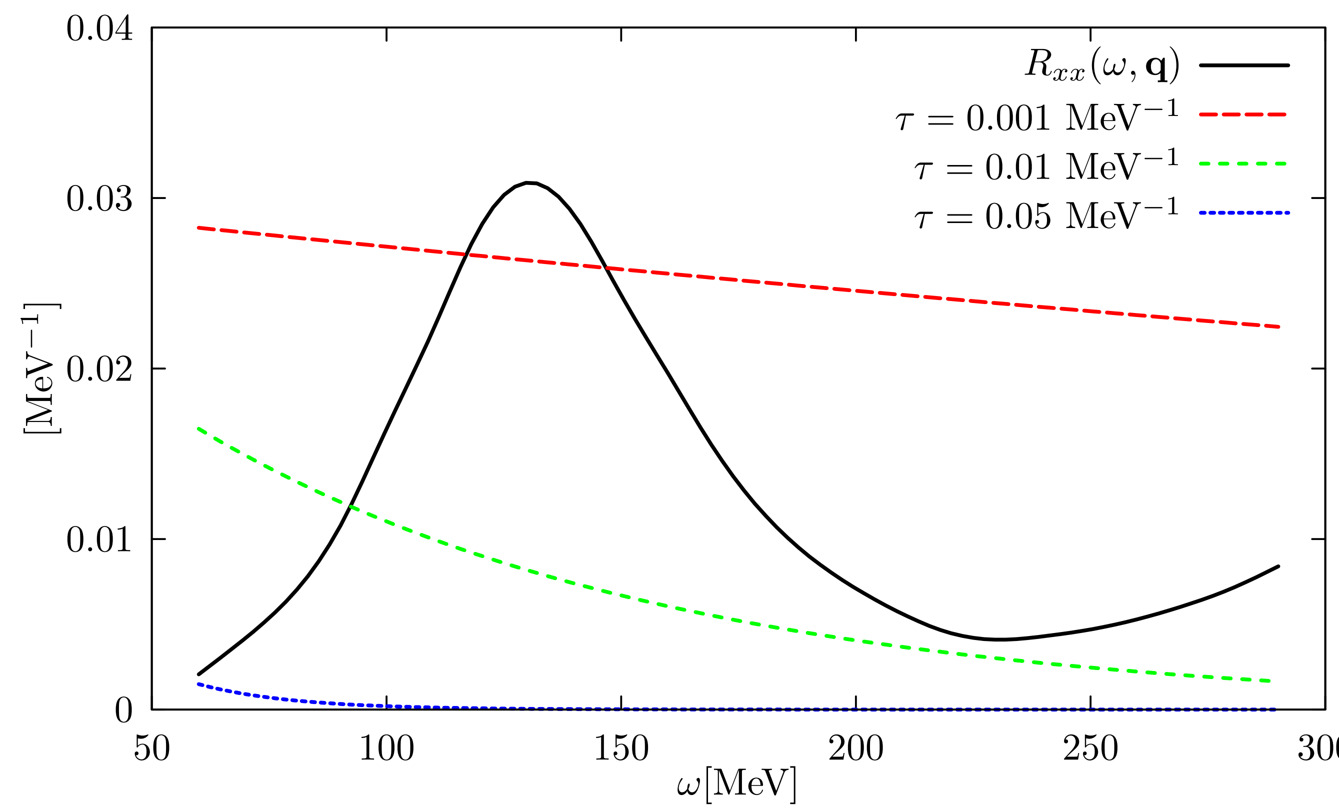

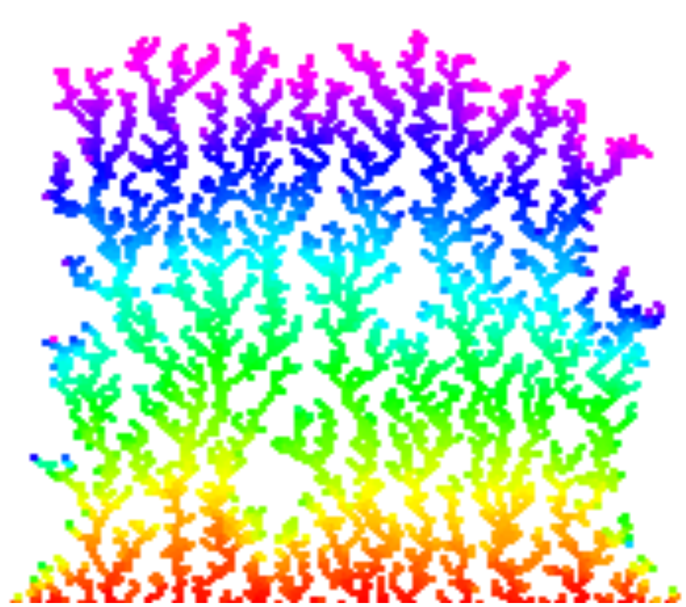

The system is first heated up by the transition operator.
Its cooling determines the Euclidean response of the system

$$E_{\alpha\beta}(\tau,\mathbf{q}) = \langle\Psi_0|J^\dagger_\alpha(\mathbf{q})e^{-(H-E_0)\tau}J_\beta(\mathbf{q})|\Psi_0\rangle$$

Same technique used in Lattice QCD, condensed matter physics…

^{12}C electromagnetic response

- We inverted the electromagnetic Euclidean response of ^{12}C
- Very good agreement with the experimental data. Small contribution from two-body currents.

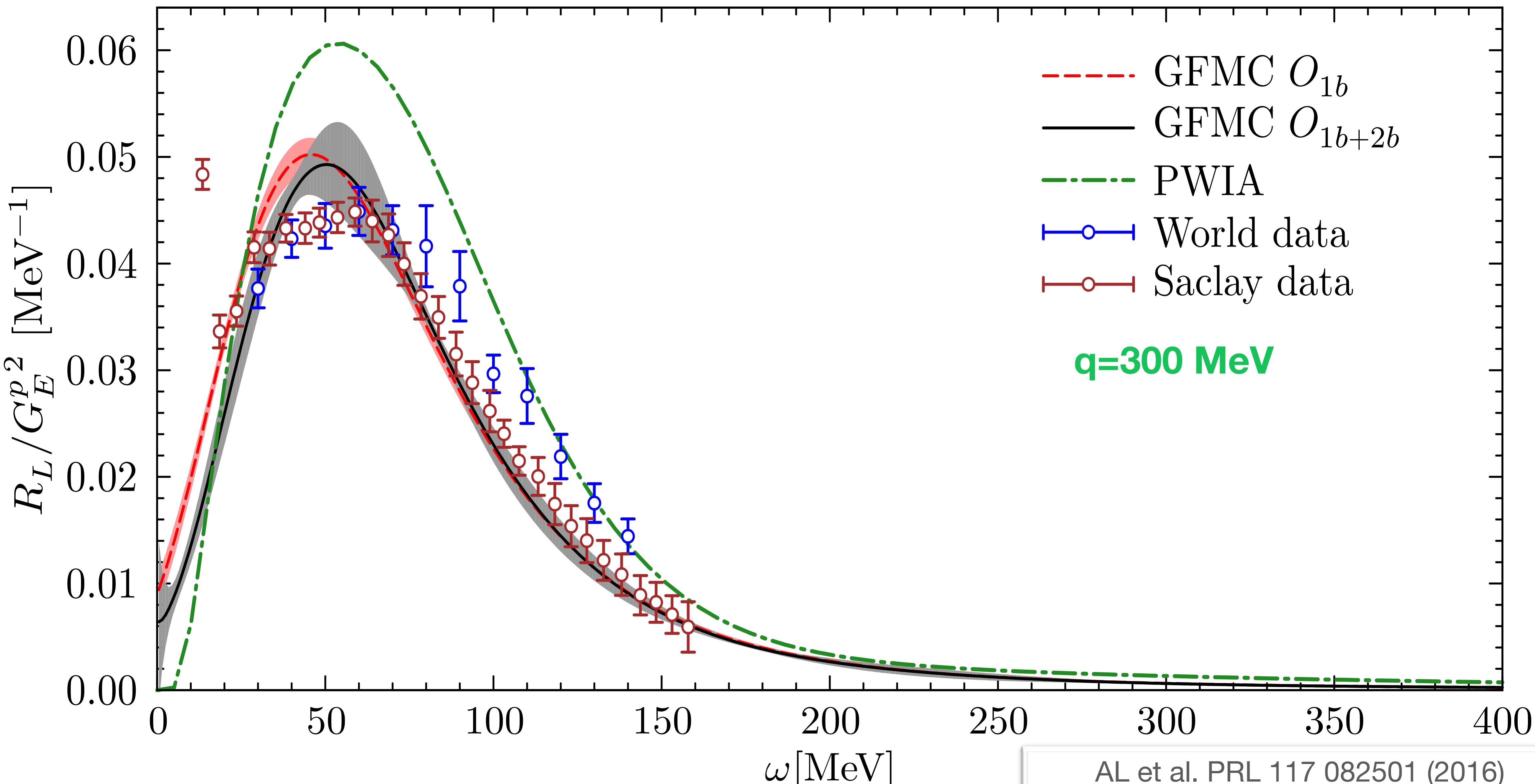

AL et al. PRL 117 082501 (2016)

^{12}C electromagnetic response

- We inverted the electromagnetic Euclidean response of ^{12}C
- Very good agreement with the experimental data. Small contribution from two-body currents.

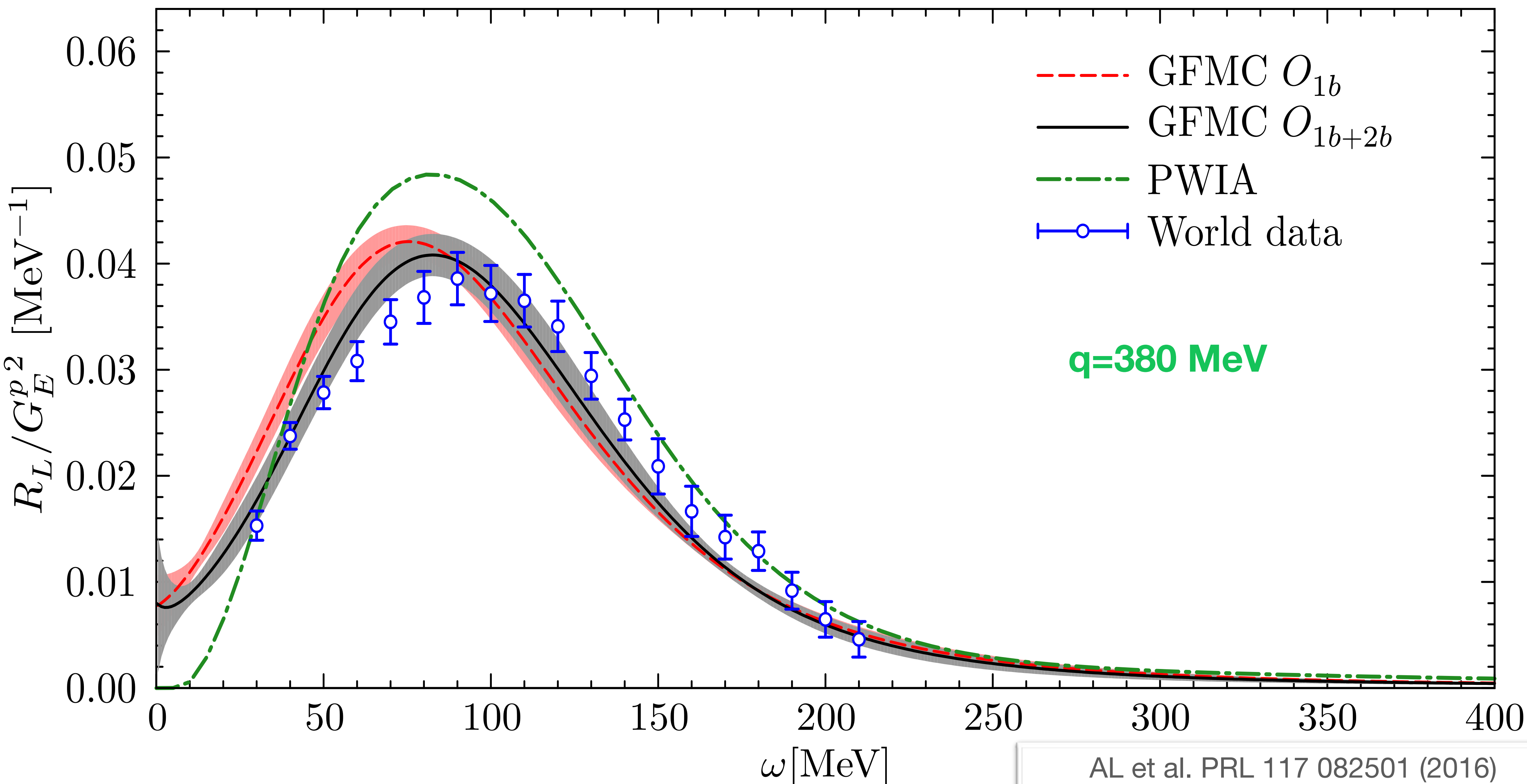

AL et al. PRL 117 082501 (2016)

^{12}C electromagnetic response

- We inverted the electromagnetic Euclidean response of ^{12}C
- Very good agreement with the experimental data. Small contribution from two-body currents.

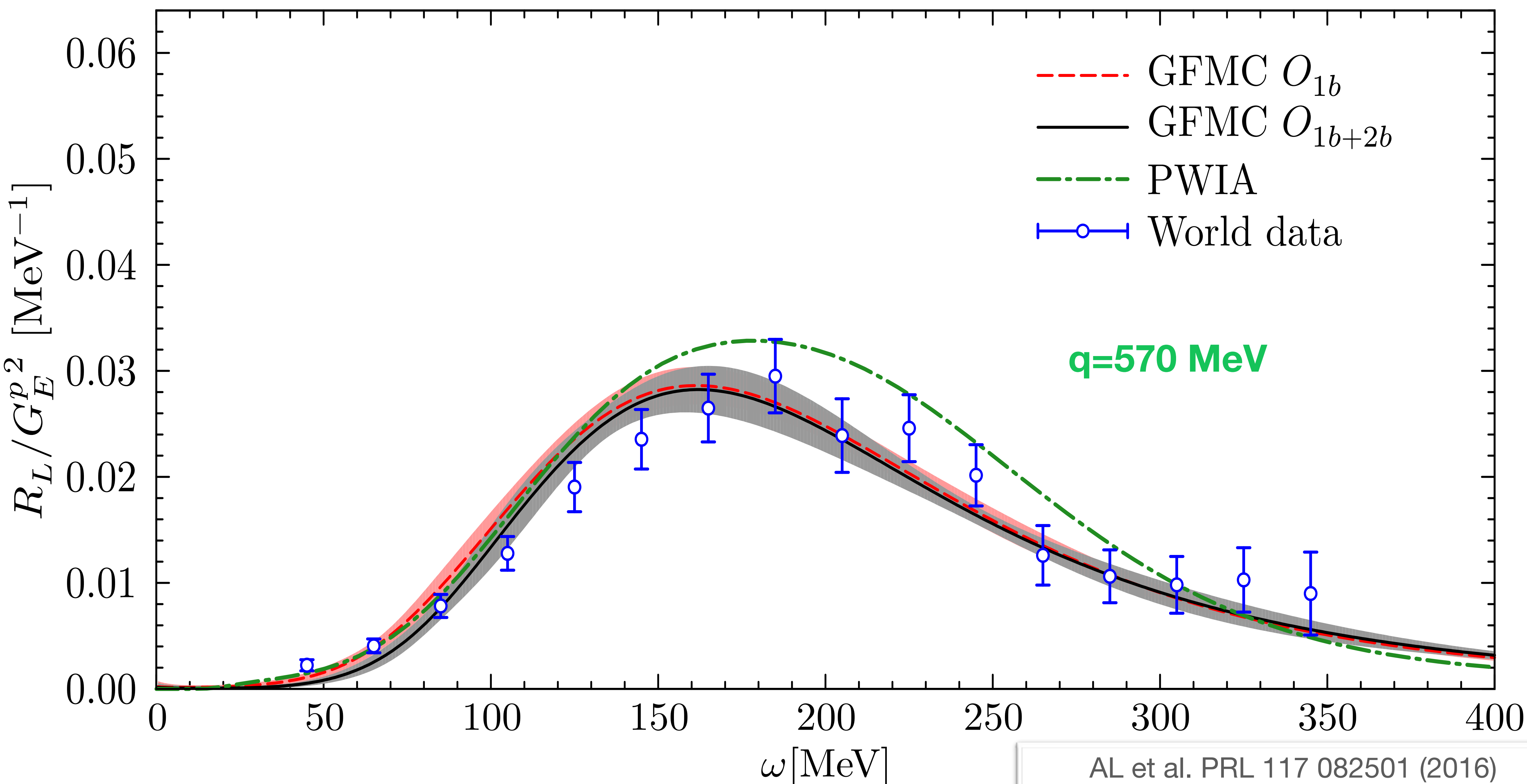

AL et al. PRL 117 082501 (2016)

^{12}C electromagnetic response

- We inverted the electromagnetic Euclidean response of ^{12}C
- Very good agreement with the experimental data once two-body currents are accounted for

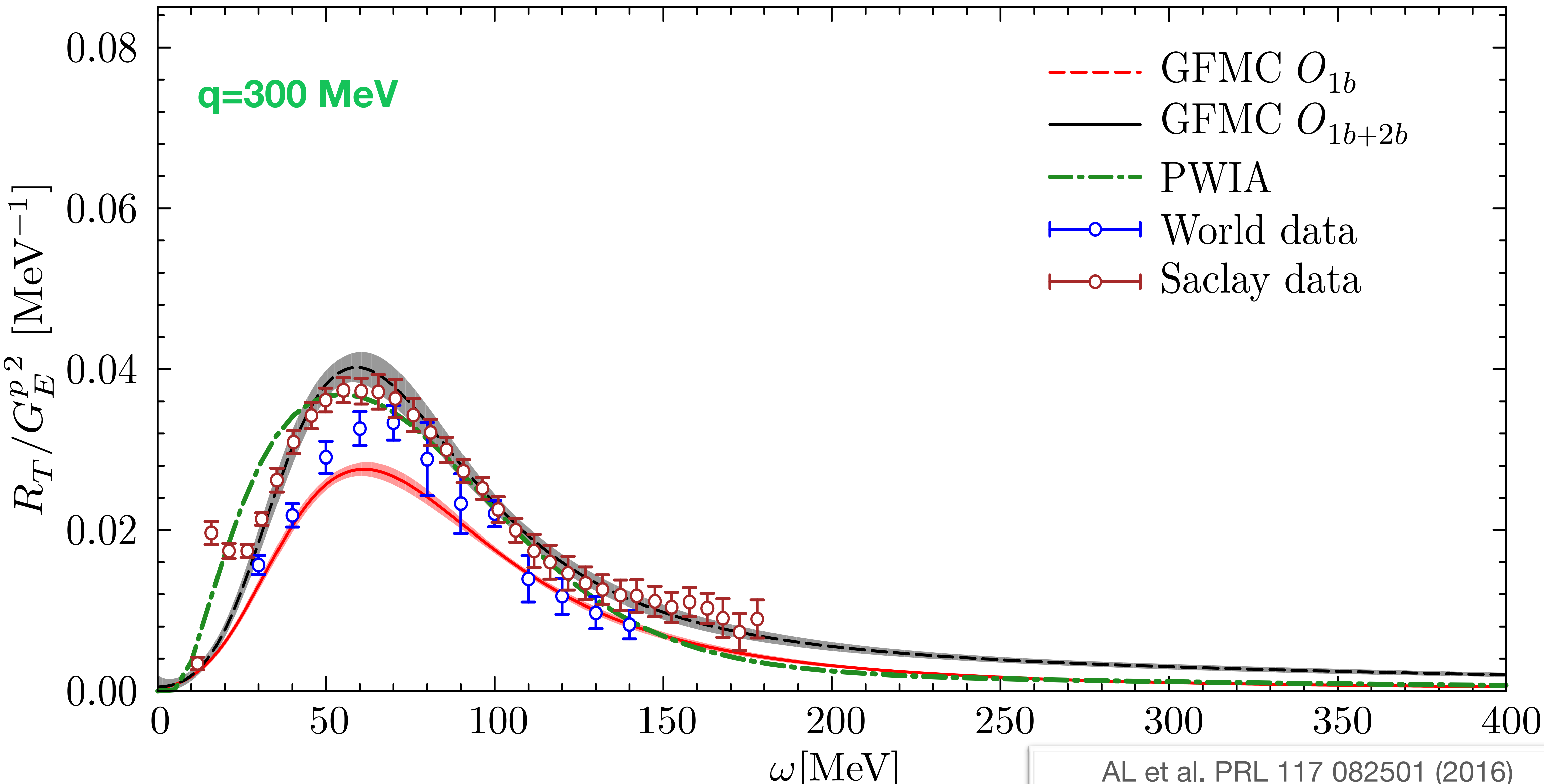

AL et al. PRL 117 082501 (2016)

^{12}C electromagnetic response

- We inverted the electromagnetic Euclidean response of ^{12}C
- Very good agreement with the experimental data once two-body currents are accounted for

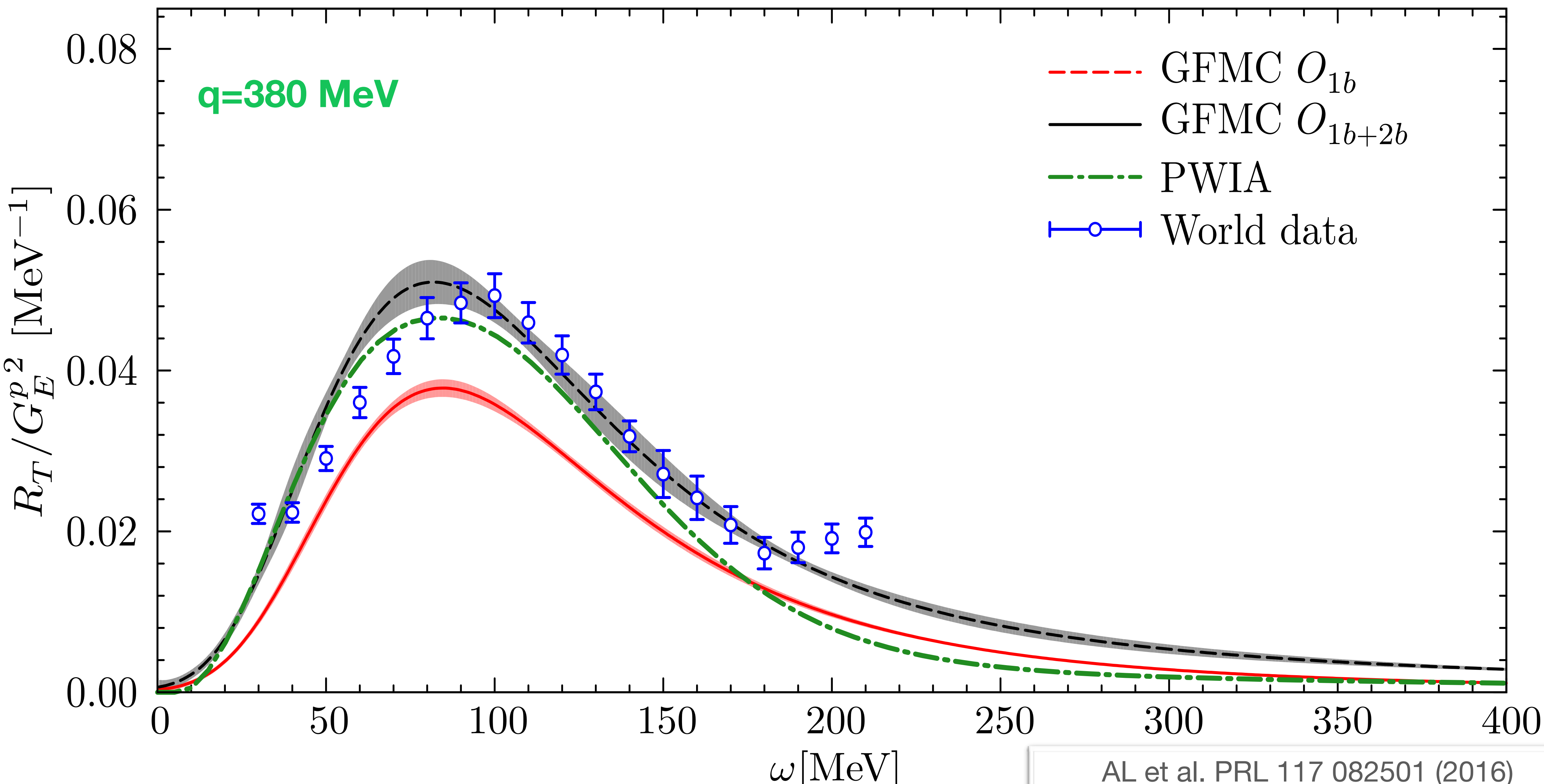

AL et al. PRL 117 082501 (2016)

^{12}C electromagnetic response

- We inverted the electromagnetic Euclidean response of ^{12}C
- Very good agreement with the experimental data once two-body currents are accounted for

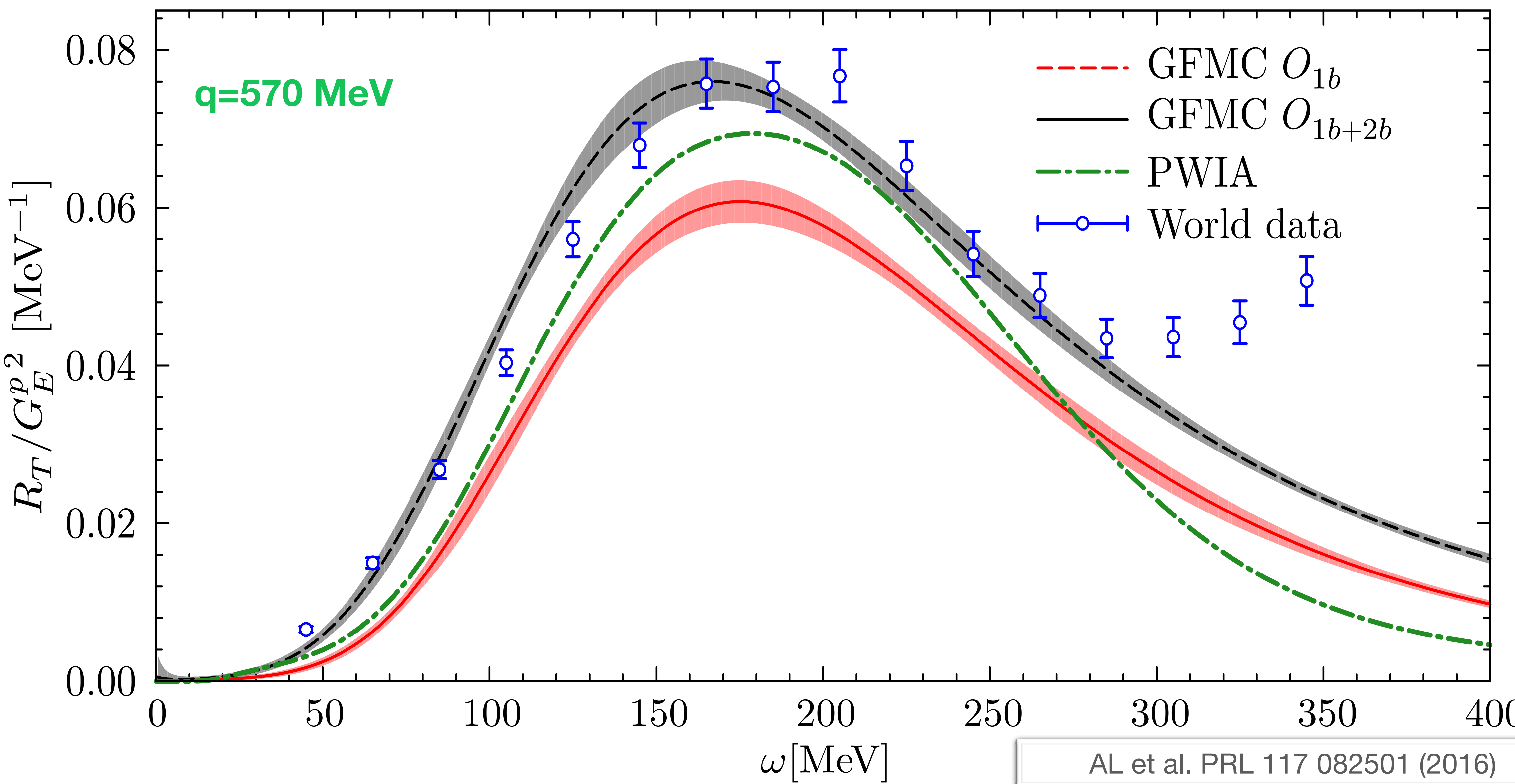

AL et al. PRL 117 082501 (2016)

^{12}C neutral-current response

- We were recently able to invert the neutral-current Euclidean responses of ^{12}C

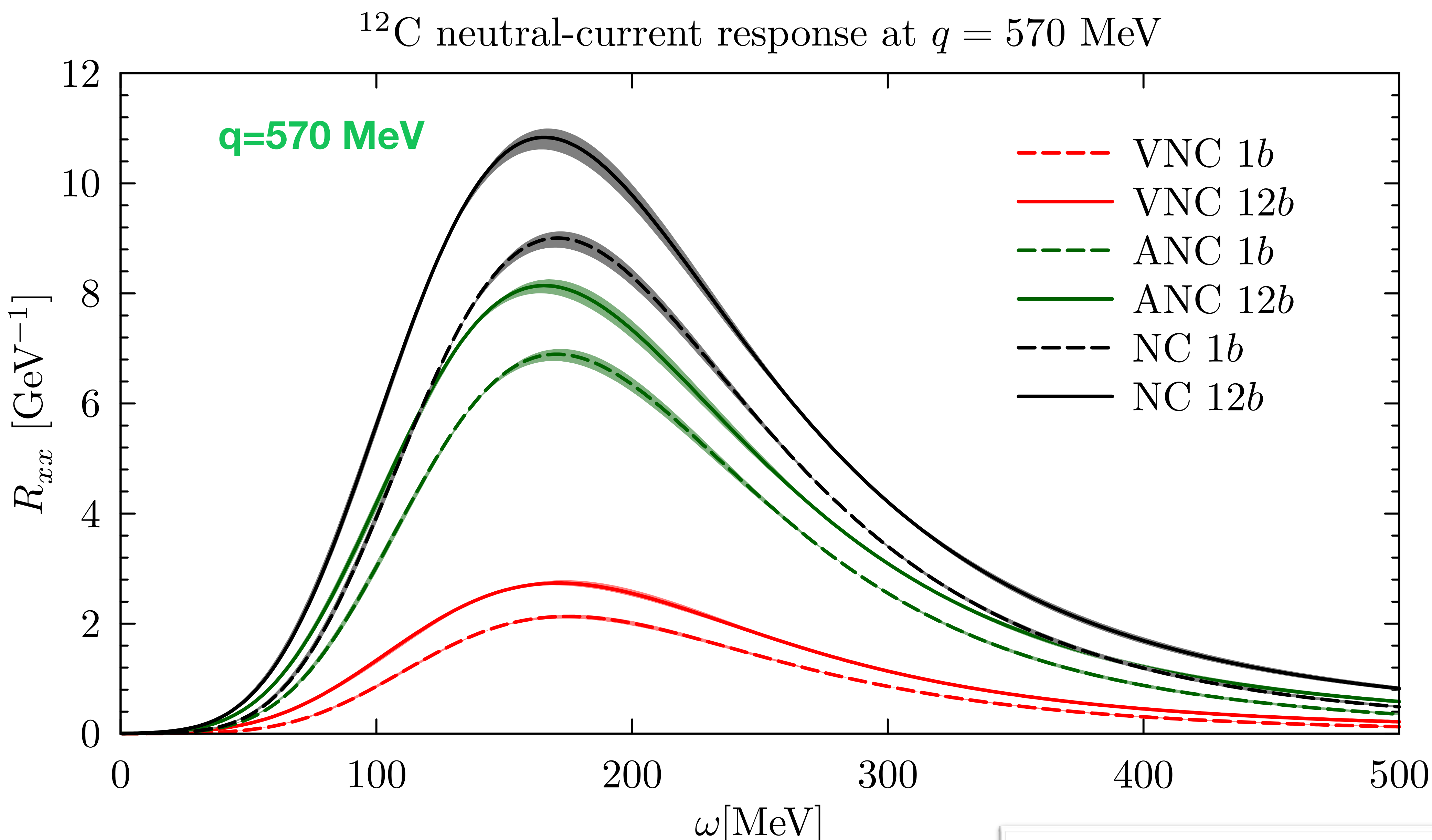

AL et al. in preparation

^{12}C neutral-current response

- We were recently able to invert the neutral-current Euclidean responses of ^{12}C

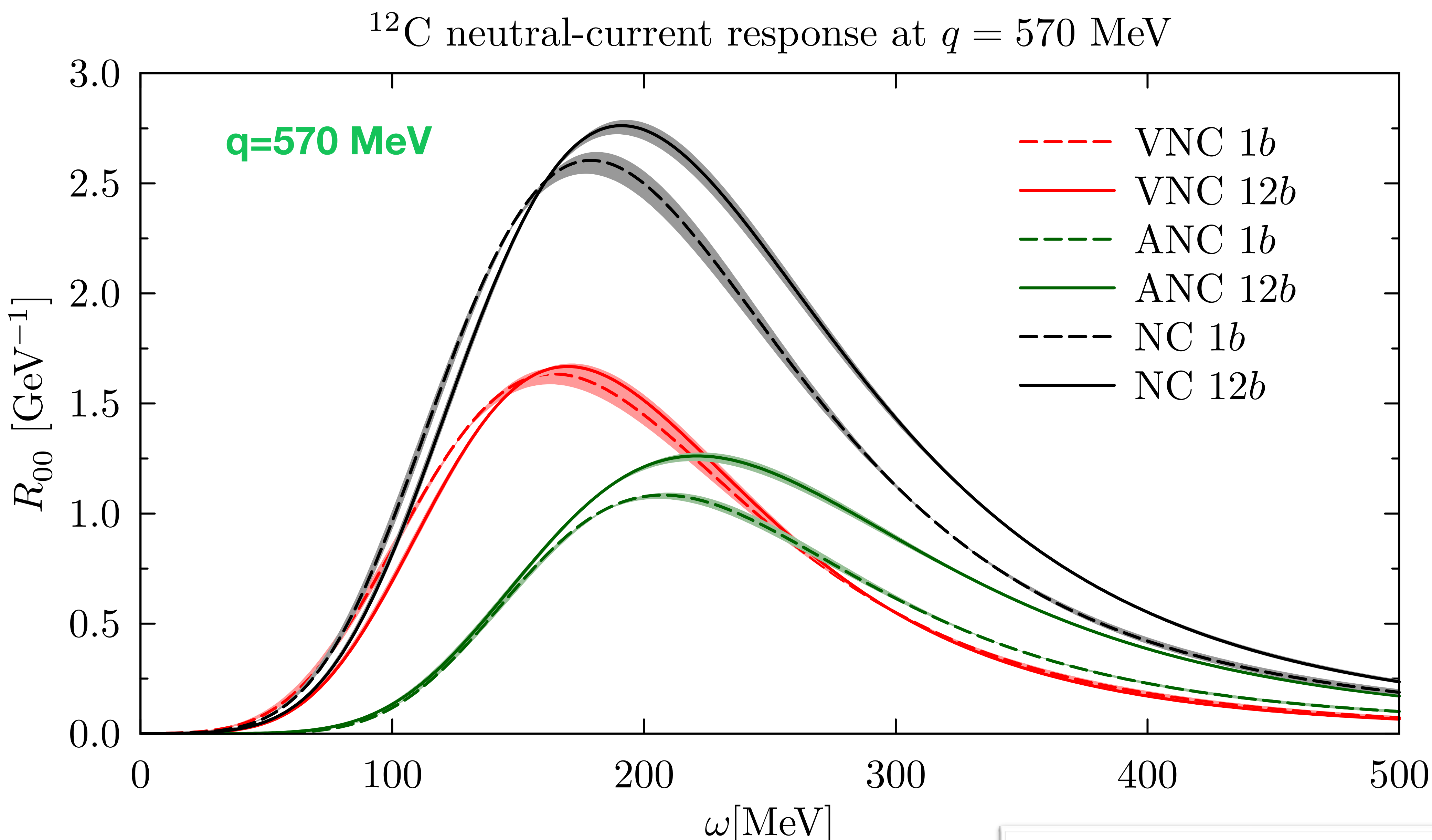

AL et al. in preparation

^{12}C neutral-current response

- We were recently able to invert the neutral-current Euclidean responses of ^{12}C

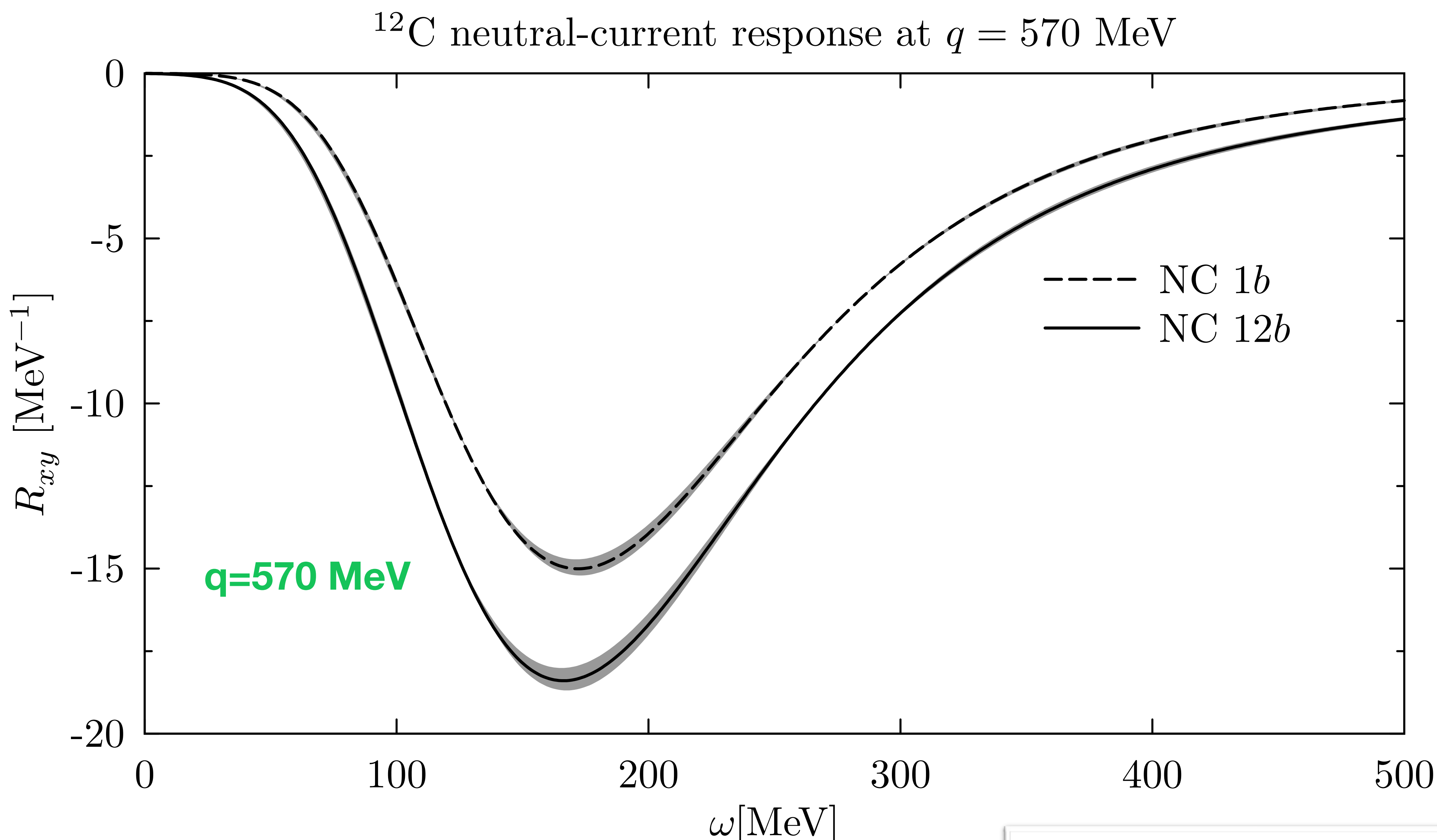

AL et al. in preparation

^{12}C neutral-current cross-section

- We also computed the neutrino and anti-neutrino differential cross sections for a fixed value of the three-momentum transfer as function of the energy transfer for a number of scattering angles

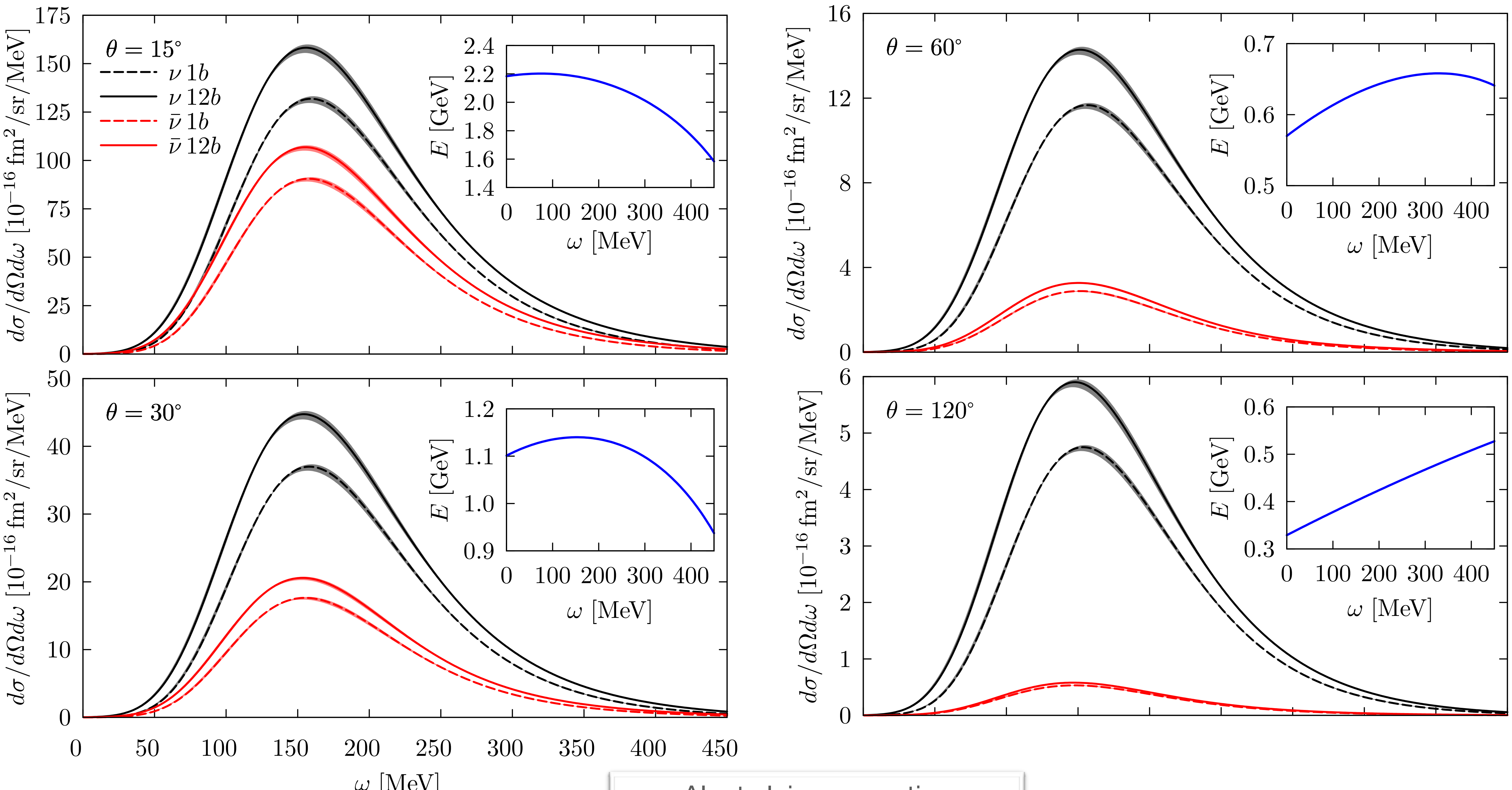

AL et al. in preparation

^{12}C neutral-current cross-section

- Because of the cancellations between the dominant contributions proportional to the R_{xx} and R_{xy} response functions, the anti-neutrino cross section decreases rapidly relative to the neutrino cross section as the scattering angle changes from the forward to the backward hemisphere

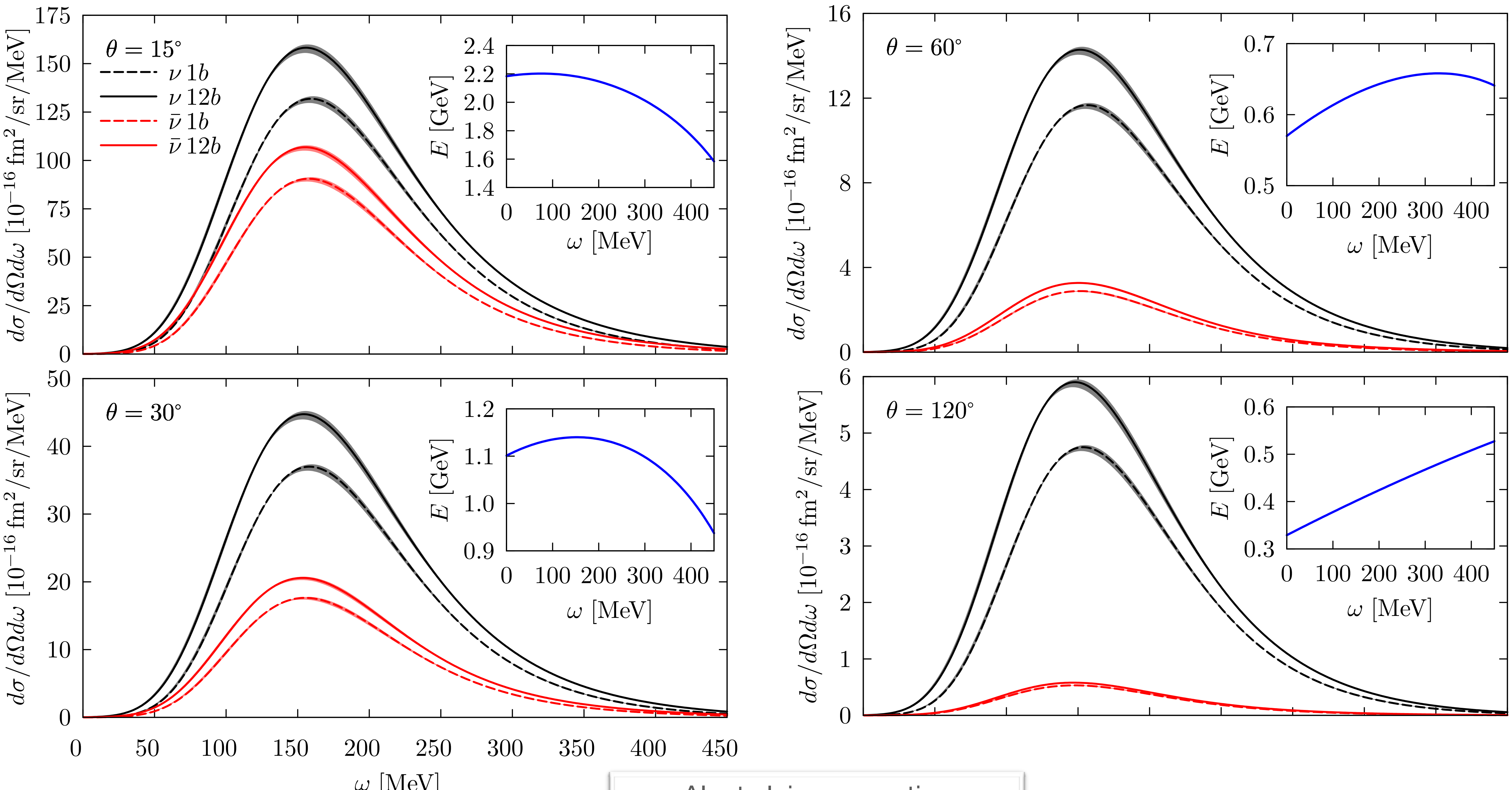

AL et al. in preparation

^{12}C neutral-current cross-section

- For this same reason, two-body current contributions are smaller for the antineutrino than for the neutrino cross section, in fact becoming negligible for the antineutrino backward-angle

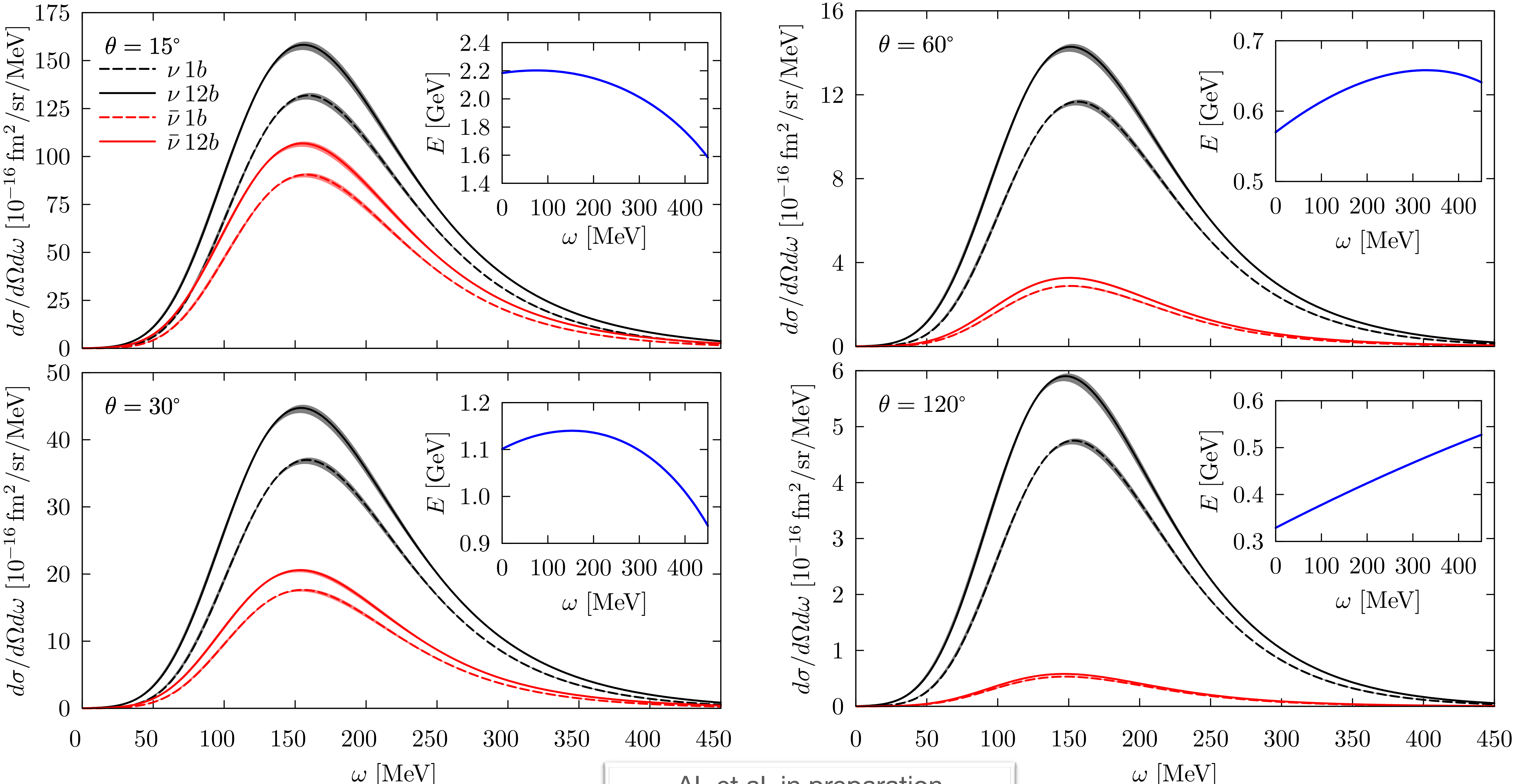

AL et al. in preparation

Scaling properties of the GFMC responses

- The experimental longitudinal response functions of ^{4}He and ^{12}C exhibit scaling of the first kind

$$f_{L,T}(\psi) = k_F \times \frac{R_{L,T}}{G_{L,T}}$$

- By properly choosing k_F, scaling of the second kind between ^{4}He and ^{12}C also occurs

- In both cases the scaling function is very different from the one of the global Fermi gas model

- The scaling functions exhibit a clearly asymmetric shape, with a tail extending in the region $\psi > 0$

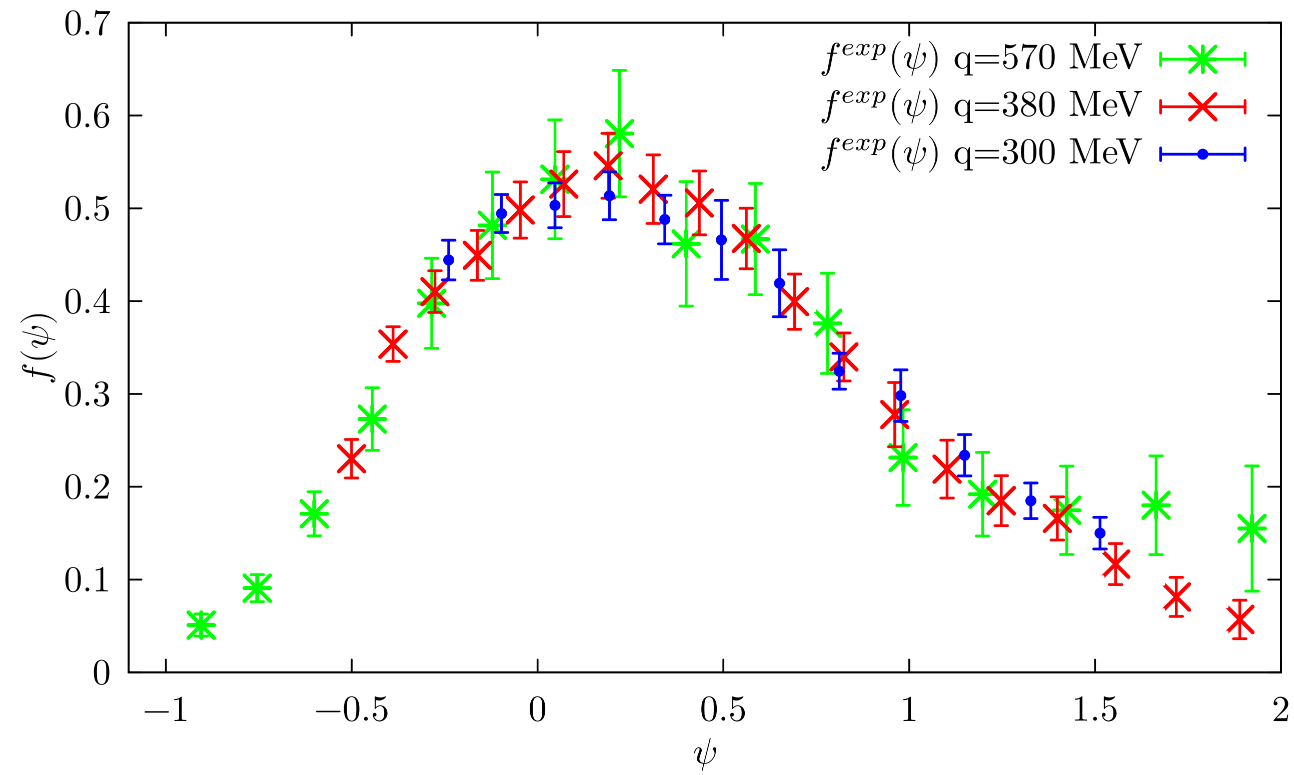

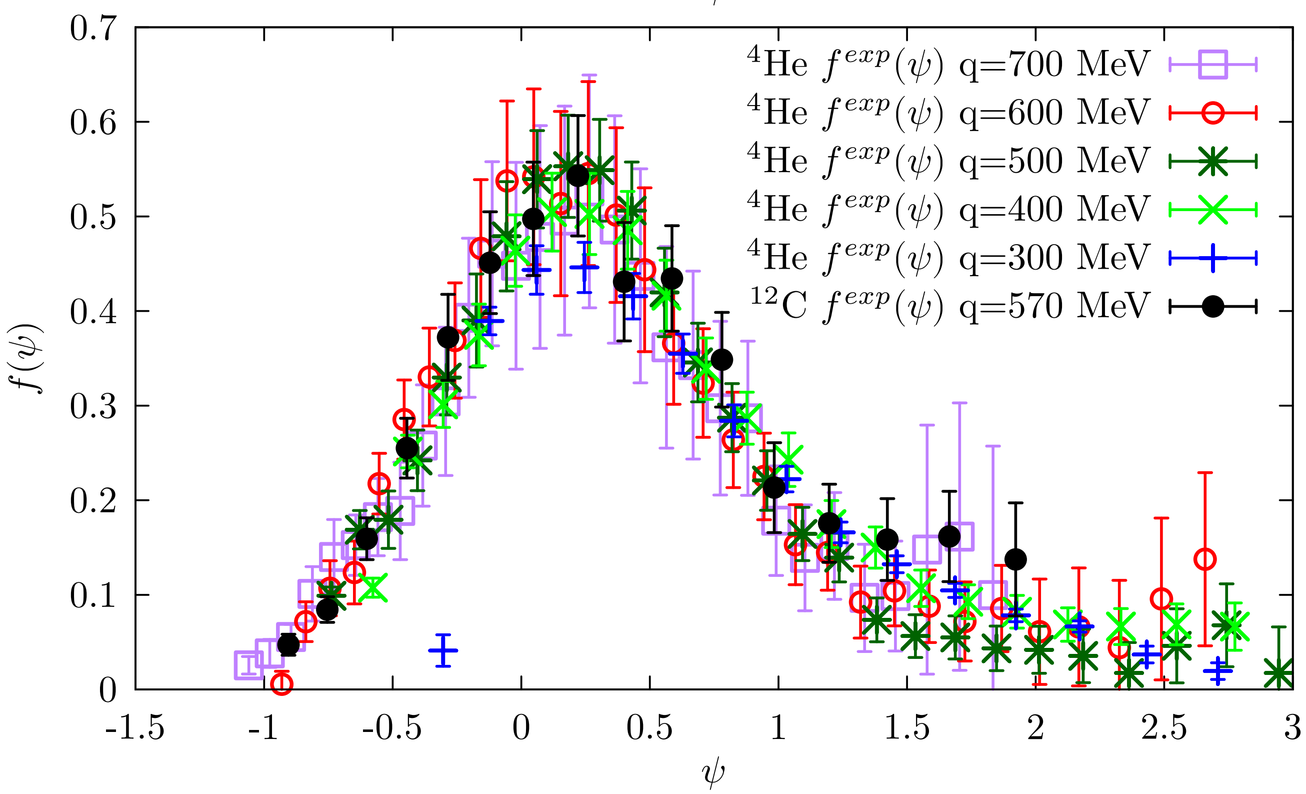

Scaling properties of the GFMC responses

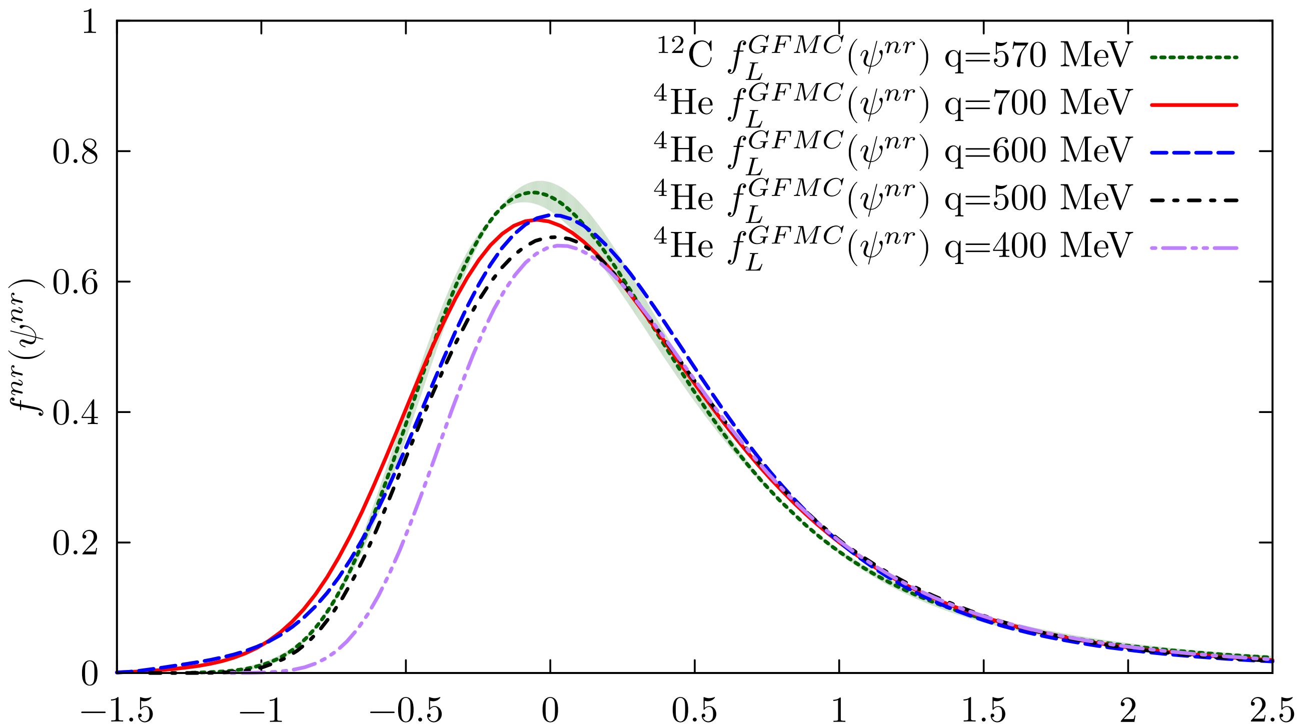

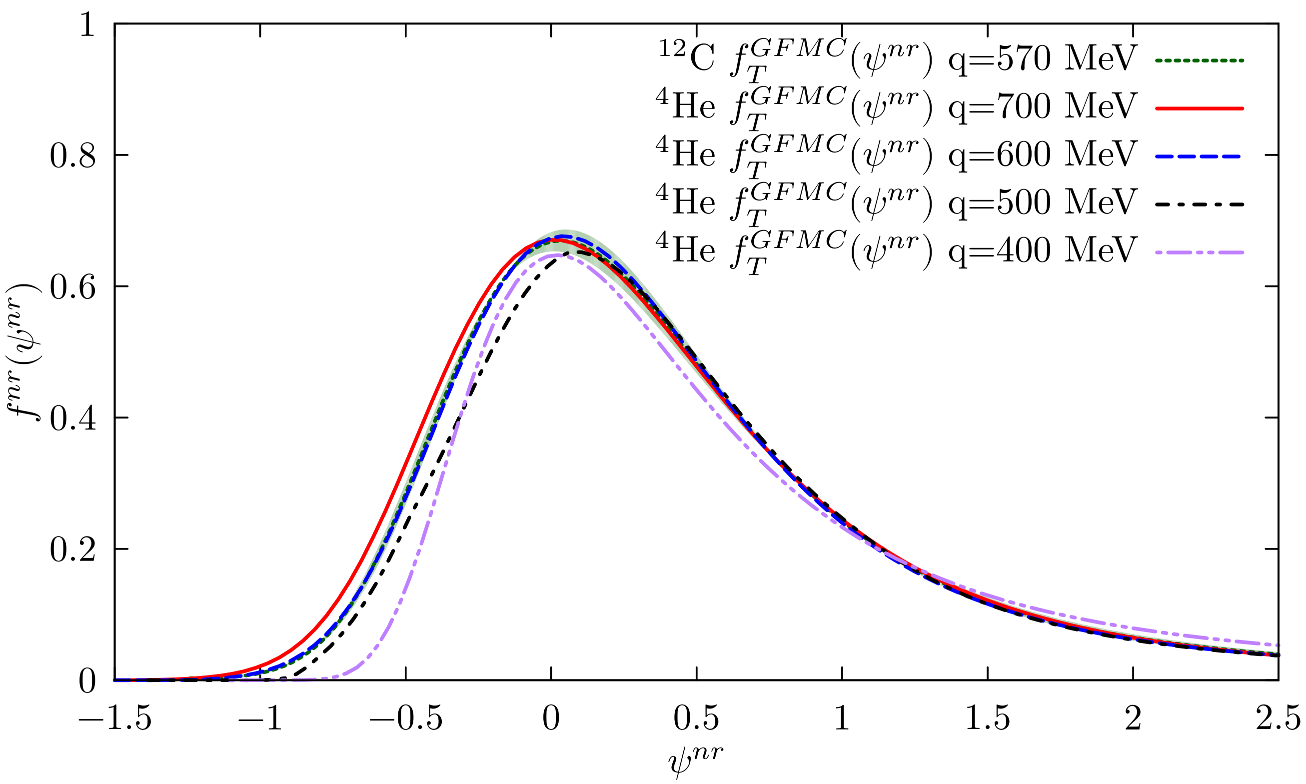

- We studied the GFMC non-relativistic scaling functions of ^{4}He and ^{12}C

$$f_{L,T}(\psi^{nr}) = k_F \times \frac{R_{L,T}}{G^{nr}_{L,T}}$$

- The results are consistent with scaling of zeroth, first and second kinds

- Despite the non relativistic nature of the calculation, all the scaling functions are strongly asymmetric, with a tail extending to the large ψ region.

N. Rocco et al. PRC 96, 015504 (2017)

Scaling properties of the GFMC responses

- We identified the longitudinal scaling function with the proton-density response

$$R_{p(n)} \equiv \sum_f \langle 0|\varrho^\dagger_{p(n)}(\mathbf{q})|f\rangle\langle f|\varrho_{p(n)}(\mathbf{q})|0\rangle\,\delta(E_0+\omega-E_f)$$

$$\varrho_{p(n)} \equiv \sum_i e^{i\mathbf{q}\cdot\mathbf{r}_i}\frac{(1\pm\tau_{i,z})}{2} \quad \longleftrightarrow \quad \varrho \simeq \sum_i e^{i\mathbf{q}\cdot\mathbf{r}_i}\left[G_E^p\frac{(1+\tau_{i,z})}{2}+G_E^n\frac{(1+\tau_{i,z})}{2}\right]$$

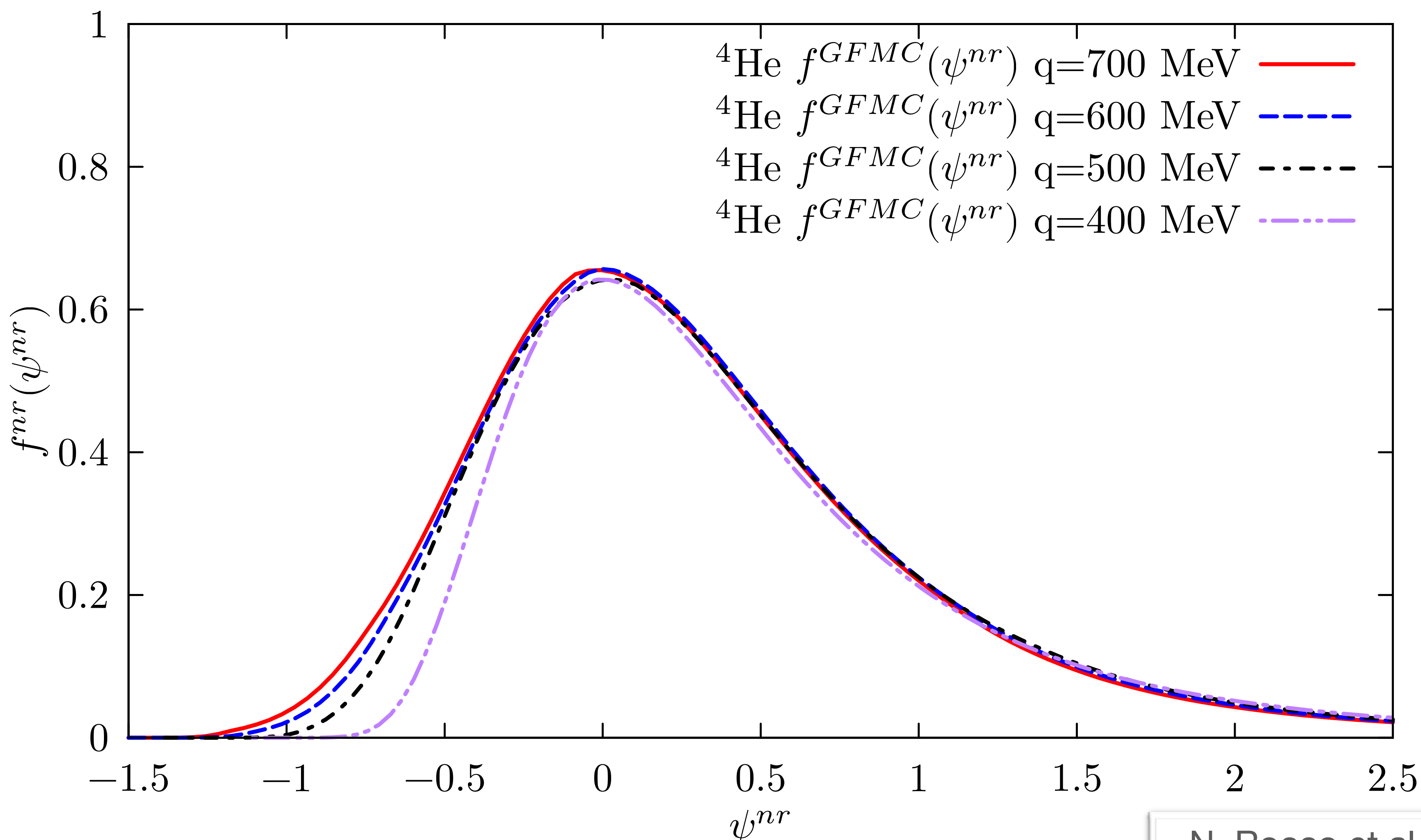

N. Rocco et al. PRC 96, 015504 (2017)

Nuclear dynamics surprises

- Beyond impulse approximation effects are important. Particularly enlightening is the comparison between the nucleon and proton responses

$$R_{N,p} \equiv \sum_f \langle 0|\rho^\dagger_{N,p}(\mathbf{q})|f\rangle\langle f|\rho_{N,p}(\mathbf{q})|0\rangle\delta(E_0+\omega-E_f)$$

$$\rho_p(\mathbf{q}) = \sum_i e^{i\mathbf{q}\mathbf{r}_i}\frac{1+\tau_{i,z}}{2} \qquad \rho_N(\mathbf{q}) = \sum_i e^{i\mathbf{q}\mathbf{r}_i} = \rho_n + \rho_p$$

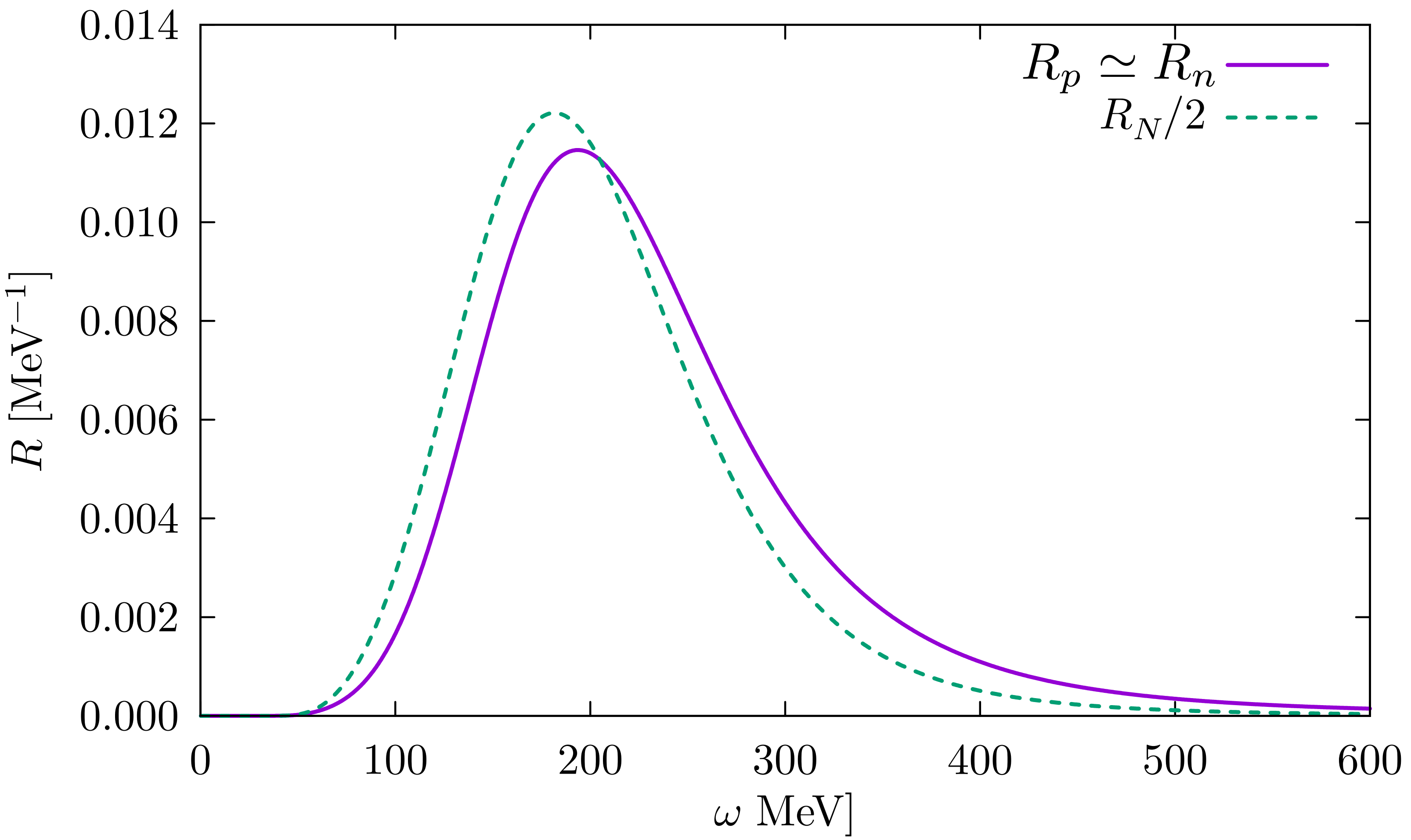

- In the impulse approximation the nucleon and the proton responses coincide

- GFMC results demonstrate the importance of the charge-exchange character of the nucleon-nucleon force

Relativistic effects in a correlated system

- Non relativistic approaches are limited to moderate momentum transfers

- In a generic reference frame the longitudinal response reads

$$R_L^{fr} = \sum_f \Big| \langle \psi_i | \sum_j \rho_j(\mathbf{q}^{fr}, \omega^{fr}) | \psi_f \rangle \Big|^2 \delta(E_f^{fr} - E_i^{fr} - \omega^{fr})$$

$$\delta(E_f^{fr} - E_i^{fr} - \omega^{fr}) \approx \delta[e_f^{fr} + (P_f^{fr})^2/(2M_T) - e_i^{fr} - (P_i^{fr})^2/(2M_T) - \omega^{fr}]$$

- The response in the LAB frame is given by the Lorentz transform

$$R_L(\mathbf{q}, \omega) = \frac{\mathbf{q}^2}{(\mathbf{q}^{fr})^2} \frac{E_i^{fr}}{M_0} R_L^{fr}(\mathbf{q}^{\mathbf{fr}}, \omega^{fr})$$

where

$$q^{fr} = \gamma(q - \beta\omega),\ \ \omega^{fr} = \gamma(\omega - \beta q),\ \ P_i^{fr} = -\beta\gamma M_0,\ \ E_i^{fr} = \gamma M_0$$

Relativistic effects in a correlated system

- The ^{4}He longitudinal response at q=700 MeV strongly depends upon the original reference frame

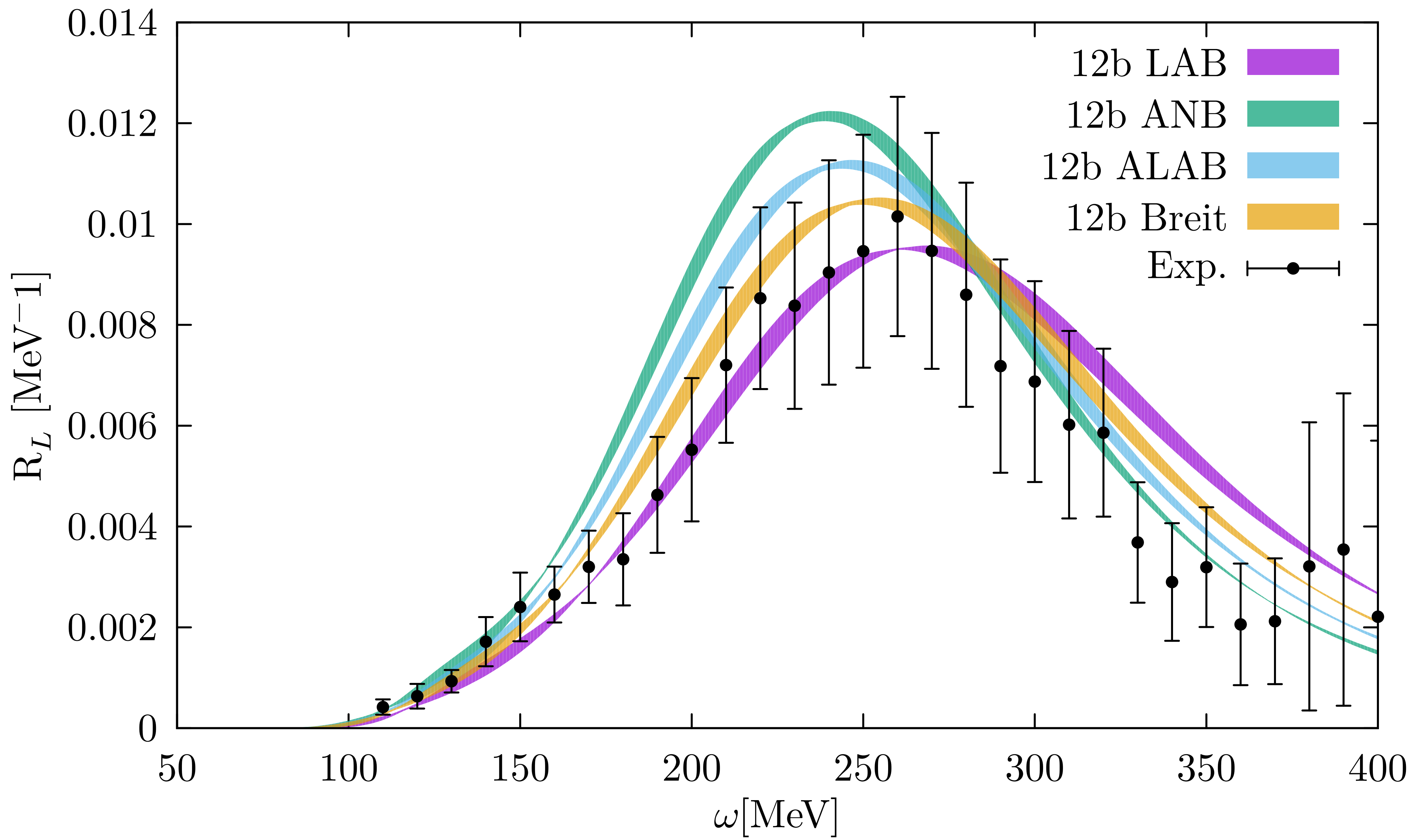

Relativistic effects in a correlated system

- To determine the relativistic corrections, we consider a two-body breakup model

$$p^{fr} = \mu\Big(\frac{p_N^{fr}}{m_N} - \frac{p_X^{fr}}{M_X}\Big) \quad \longleftrightarrow \quad \mu = \frac{m_N M_X}{m_N + M_X}$$

$$P_f^{fr} = p_N^{fr} + p_X^{fr}$$

- The relative momentum is derived in a relativistic fashion

$$\omega^{fr} = E_f^{fr} - E_i^{fr}$$

$$E_f^{fr} = \sqrt{m_N^2 + [\mathbf{p}^{fr} + \mu/M_X \mathbf{P}_f^{fr}]^2} + \sqrt{M_X^2 + [\mathbf{p}^{fr} - \mu/m_N \mathbf{P}_f^{fr}]^2}$$

- And it is used as input in the non relativistic kinetic energy

$$e_f^{fr} = (p^{fr})^2/(2\mu)$$

- The energy-conserving delta function reads

$$\delta(E_f^{fr} - E_i^{fr} - \omega^{fr}) = \delta(F(e_f^{fr}) - \omega^{fr}) = \Big(\frac{\partial F^{fr}}{\partial e_f^{fr}}\Big)^{-1} \delta[e_f^{fr} - e_f^{rel}(q^{fr}, \omega^f)]$$

Relativistic effects in a correlated system

- The ^{4}He longitudinal response at q=700 MeV mildly depends upon the original reference frame

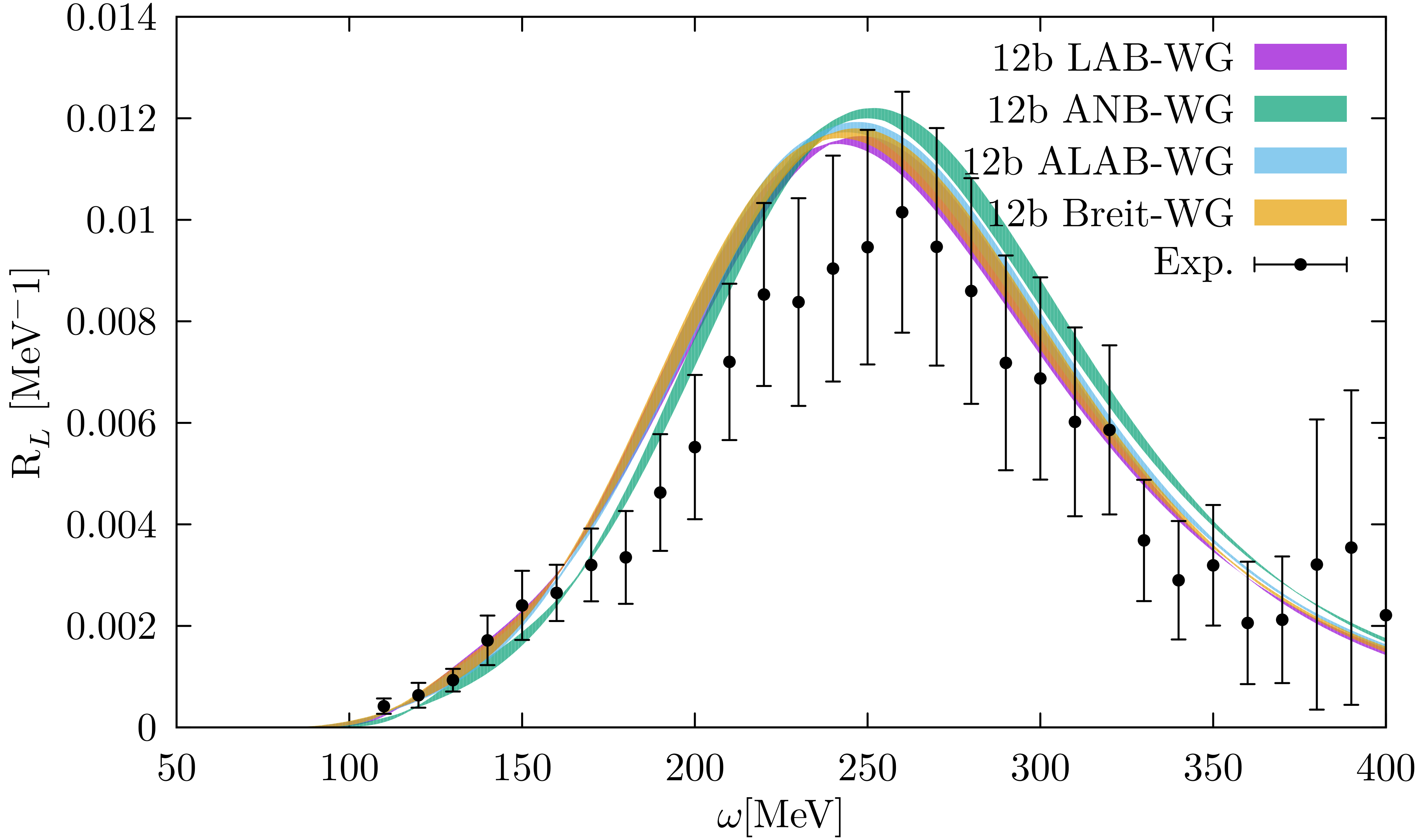

Relativistic effects in a correlated system

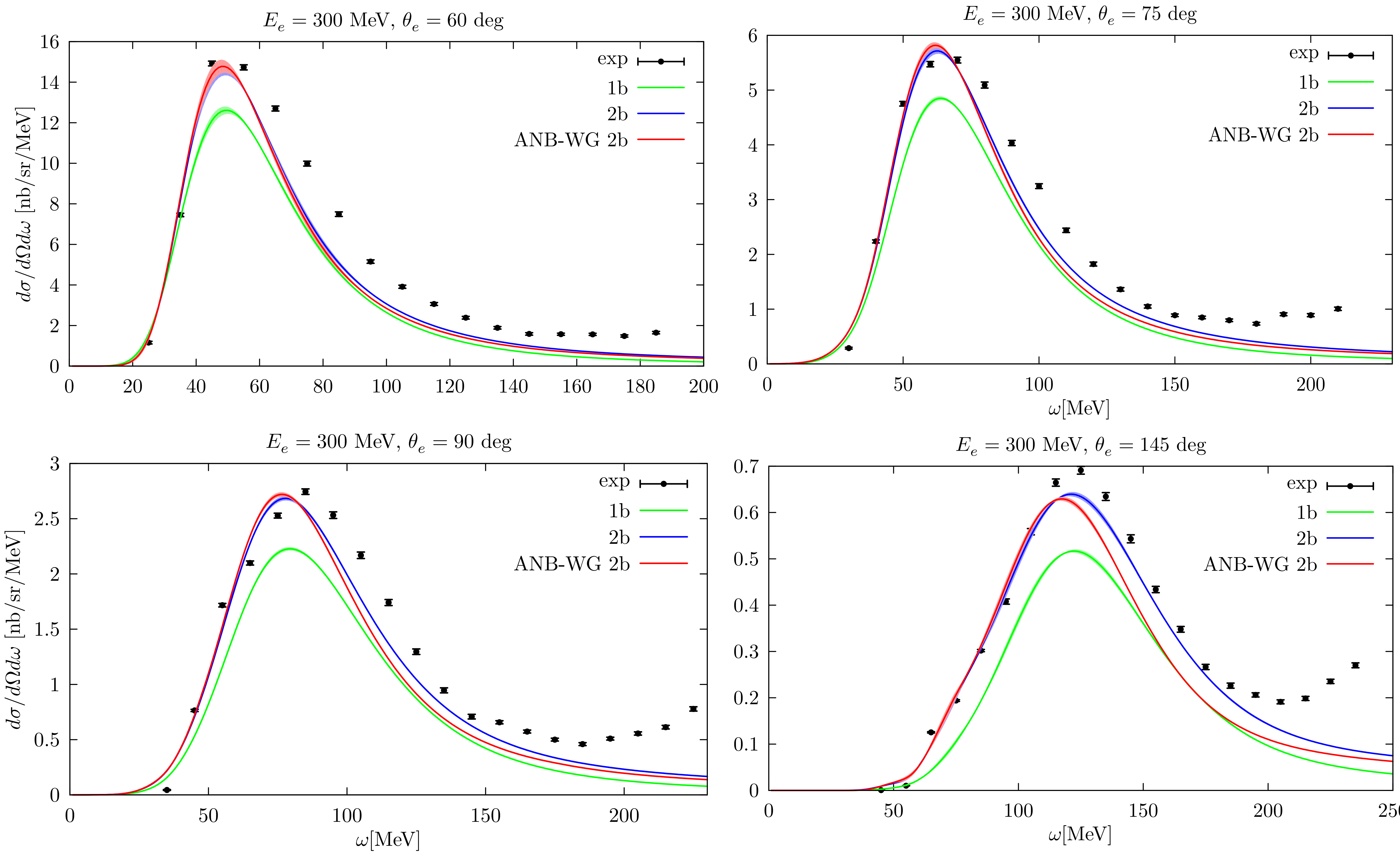

Relativistic effects in a correlated system

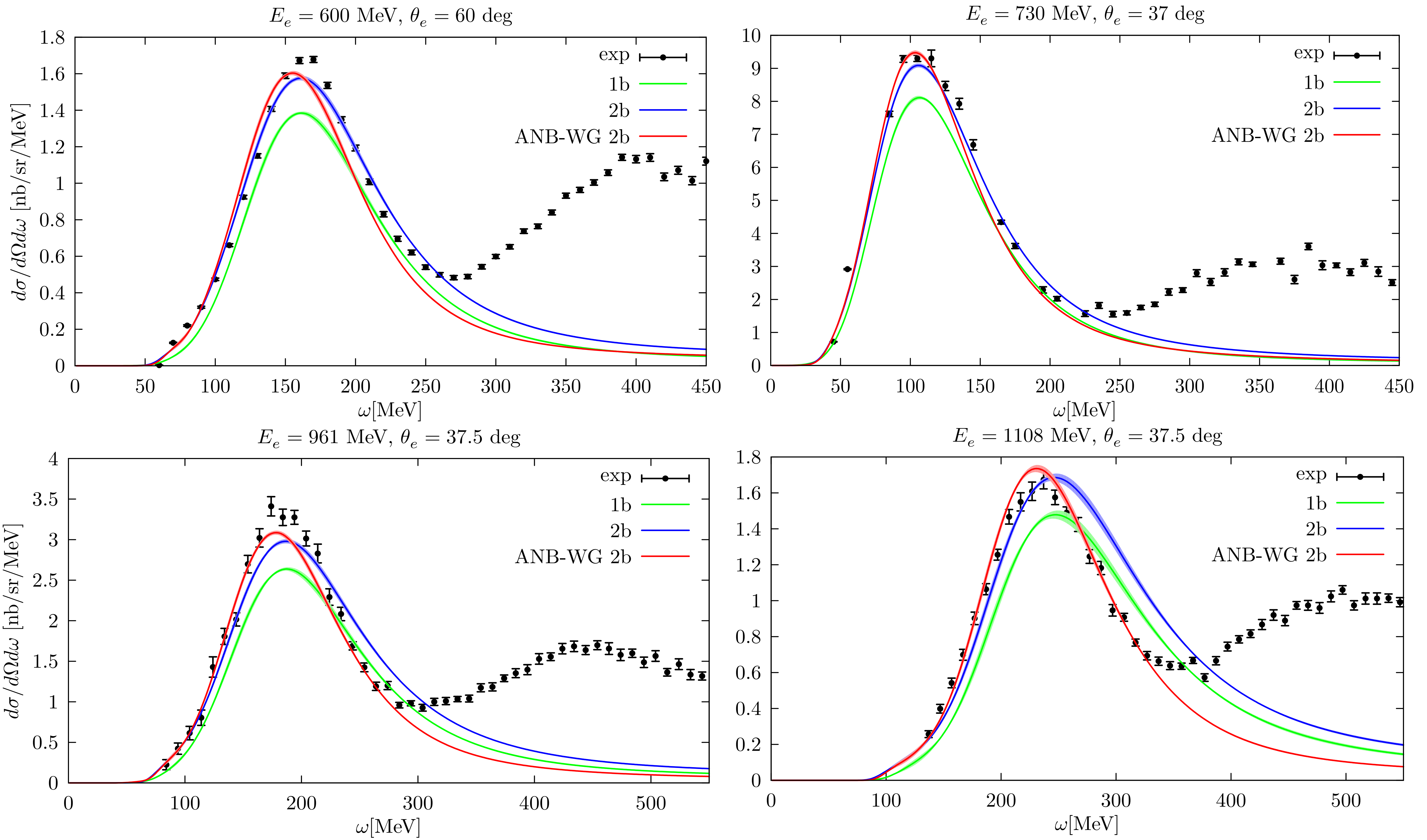

Conclusions

- The two-body currents enhancement is effective in the entire energy transfer domain.

- ^{4}He and ^{12}C results for the electromagnetic response obtained using Maximum Entropy technique are in very good agreement with experimental data.

- Two-body current contributions enhance the longitudinal and transverse axial responses

- Quantum Monte Carlo is suitable to compute cross-sections, not only responses

- Most of the relativistic effects are accounted for

Disclaimer

- The continuity equation only constraints the longitudinal components of the current

- The transverse component and the axial terms are phenomenological (the coupling constant is fitted on the tritium beta-decay)

- Two- and three- body forces not fully consistent

The theoretical error arising from modeling the nuclear dynamics cannot be properly assessed

Chiral EFT

In chiral-EFT, the symmetries of quantum chromodynamics, in particular its approximate chiral symmetry, are employed to systematically constrain classes of Lagrangians describing the interactions of baryons with pions and the interactions of these hadrons with electroweak fields

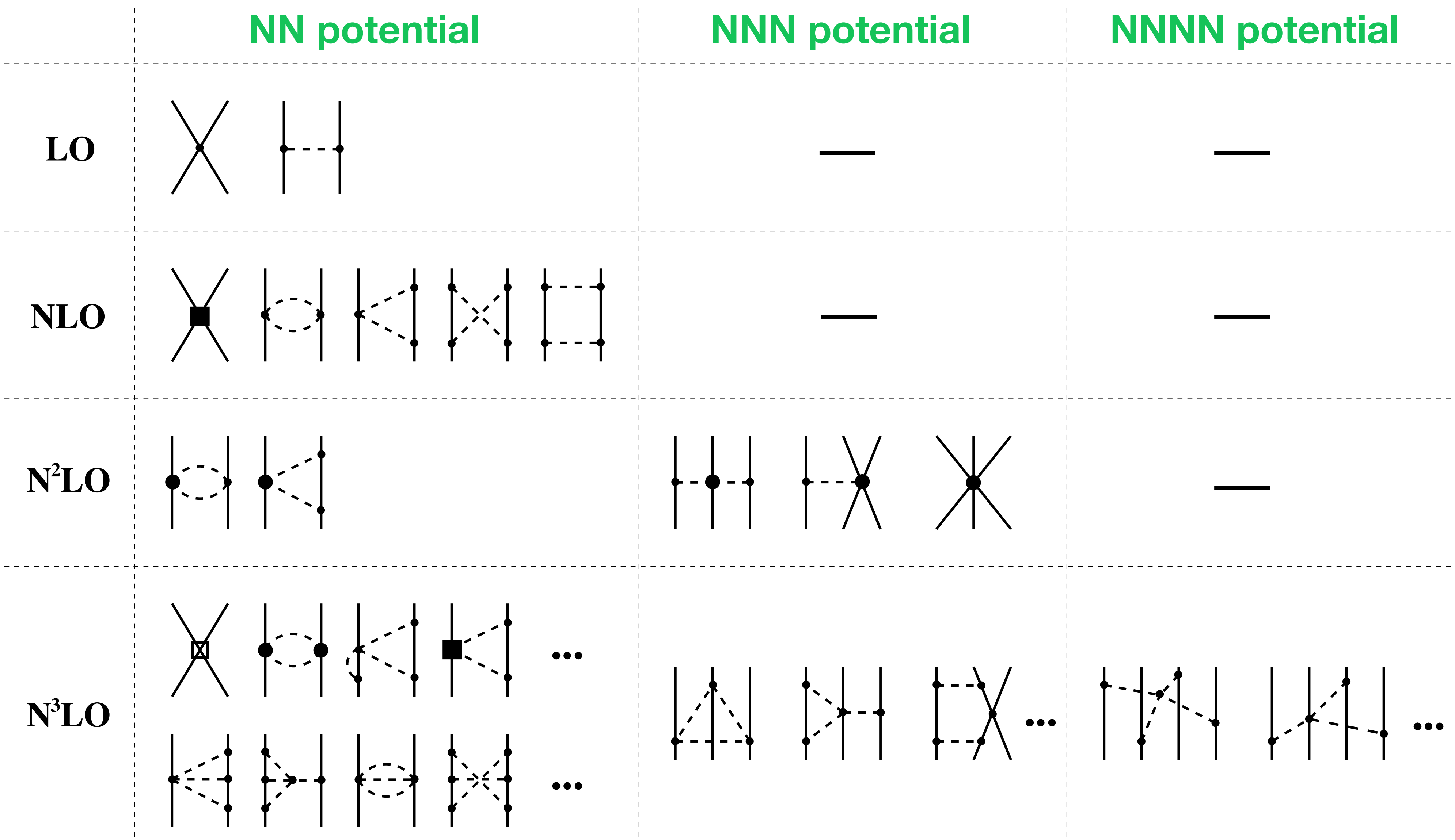

M. Piarulli et al. PRC 94 (2016) 054007

Δ-full local chiral potential

We have complemented the historical "Argonne" approach by considering a local chiral Δ -full potential giving an excellent fit to the NN scattering data that can be readily used in QMC.

- Closer connection with QCD
- Consistent MEC being constructed
- Reliable theoretical uncertainty estimation

model	order	E_{Lab} (MeV)	N_{pp+np}	χ^2/datum
b	LO	0–125	2558	59.88
b	NLO	0–125	2648	2.18
b	N2LO	0–125	2641	2.32
b	N3LO	0–125	2665	1.07
a	N3LO	0–125	2668	1.05
c	N3LO	0–125	2666	1.11
$\widetilde{a}$	N3LO	0–200	3698	1.37
$\widetilde{b}$	N3LO	0–200	3695	1.37
$\widetilde{c}$	N3LO	0–200	3693	1.40

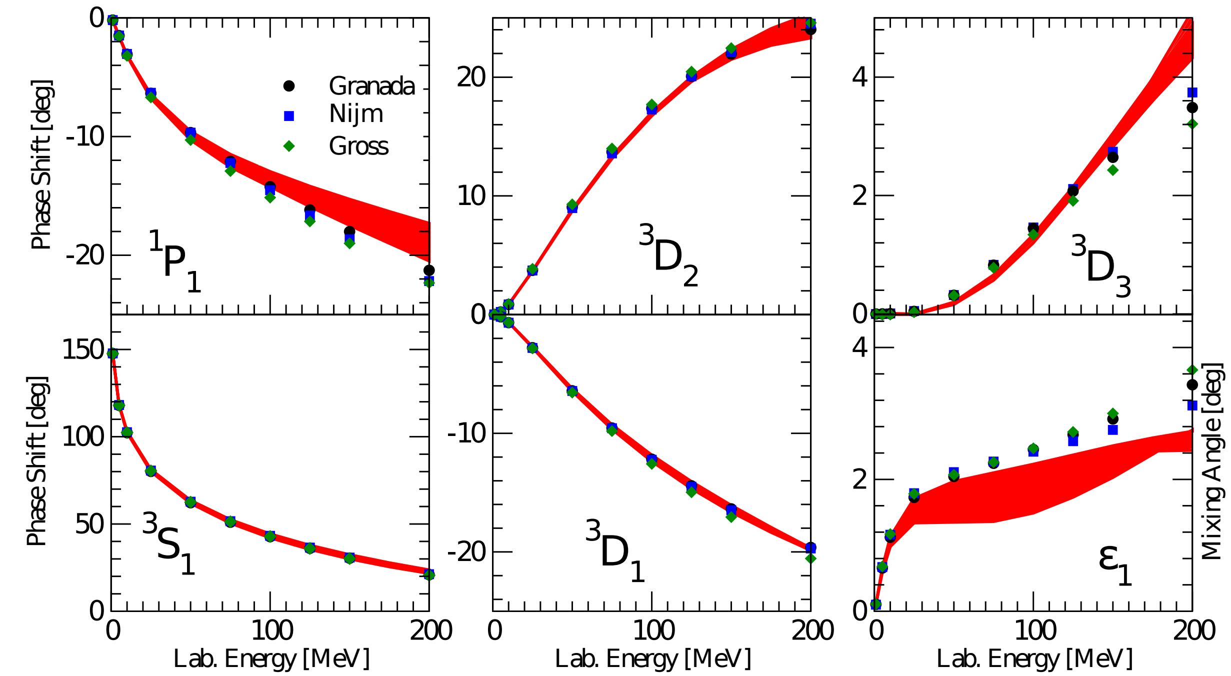

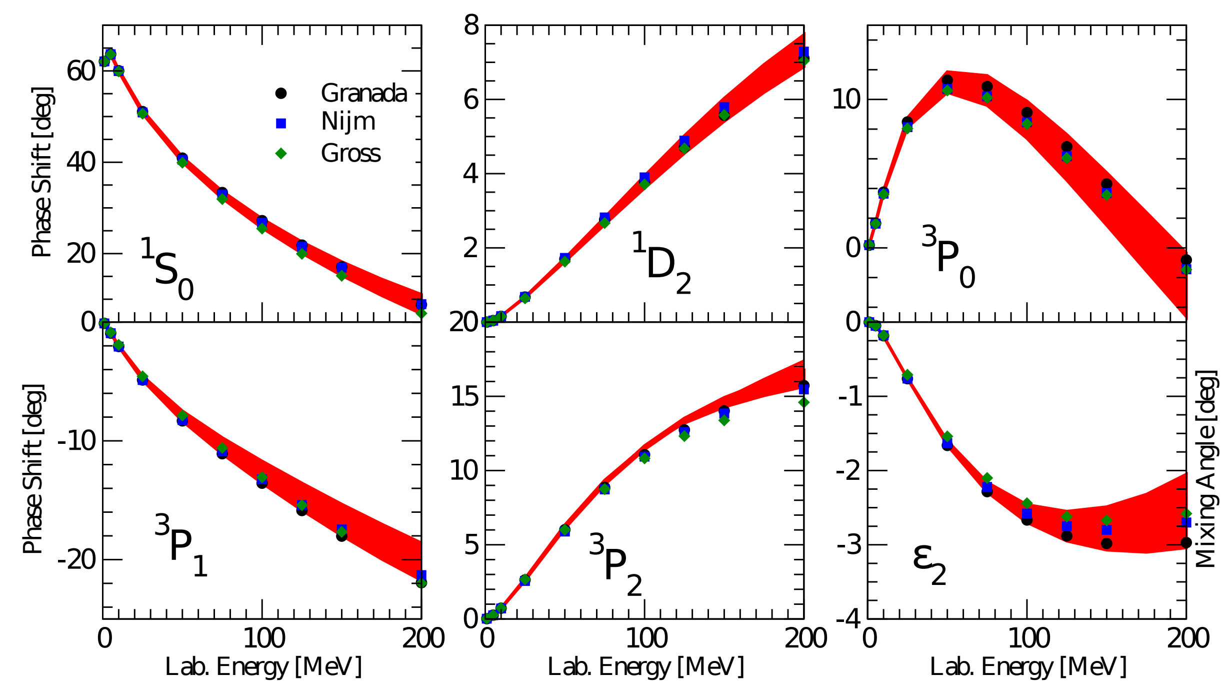

M. Piarulli, et al. arXiv:1707.02883 [nucl-th]

Δ-full local chiral potential

The experimental A≤12 ground- and excited state energies are very well reproduced by the local Δ-full NN+NNN chiral interaction

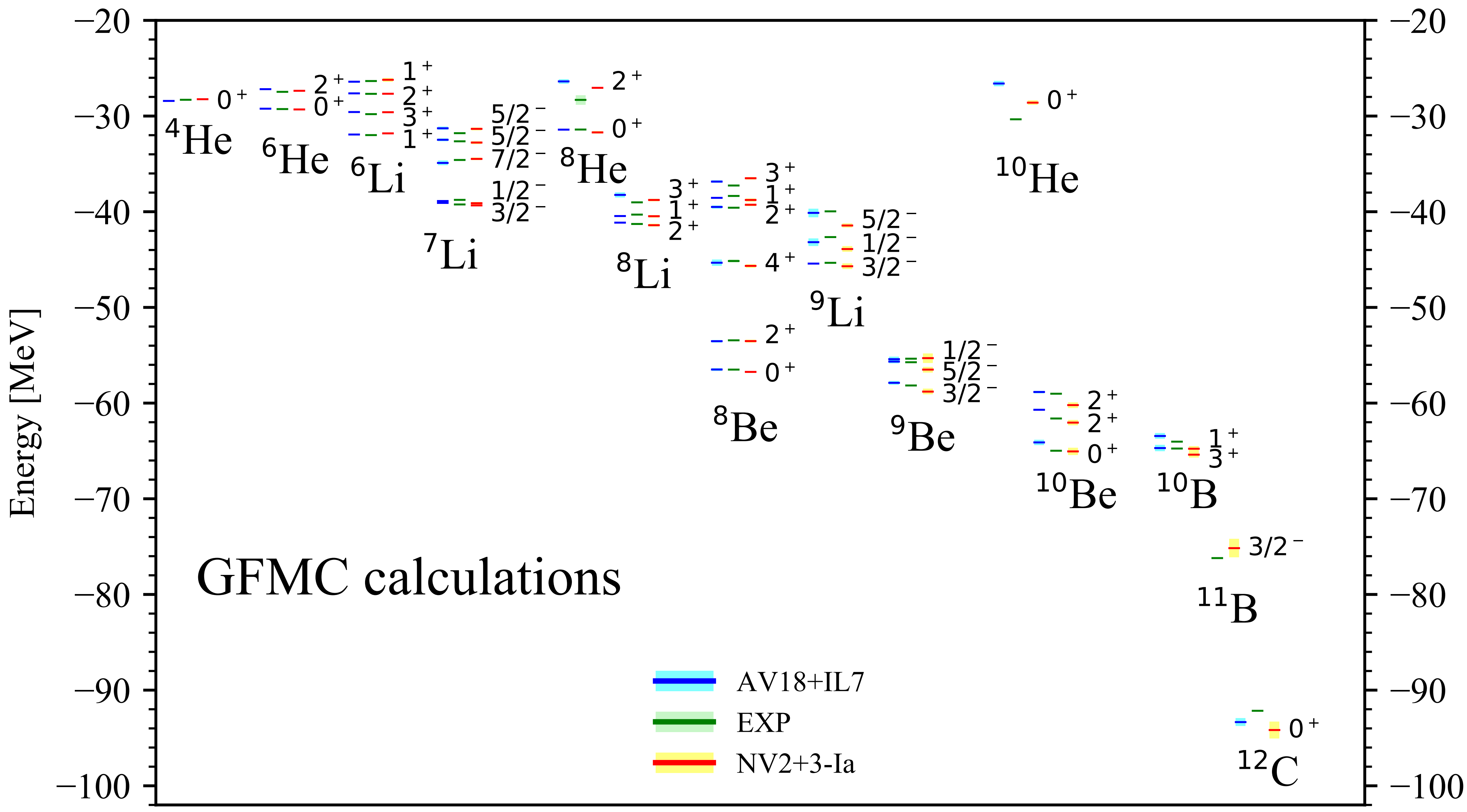

Thank you